(12) INTERNATIONAL APPLICATION PUBLISHED UNDER THE PATENT COOPERATION TREATY (PCT)

(19) World Intellectual Property Organization
International Bureau

(43) International Publication Date
11 September 2009 (11.09.2009)

PCT

(10) International Publication Number
WO 2009/111470 A2

(51) International Patent Classification:
A61K 49/00 (2006.01)

(21) International Application Number:
PCT/US2009/035875

(22) International Filing Date:
3 March 2009 (03.03.2009)

(25) Filing Language: English

(26) Publication Language: English

(30) Priority Data:
61/067,891 3 March 2008 (03.03.2008) US

(71) Applicant *(for all designated States except US)*: **KANSAS STATE UNIVERSITY RESEARCH FOUNDATION** [US/US]; 2005 Research Park Circle, Suite 105, Manhattan, KS 66502 (US).

(72) Inventors; and

(75) Inventors/Applicants *(for US only)*: **BOSSMANN, Stefan, H.** [DE/US]; 4915 Lakewood Drive, Manhattan, KS 66503 (US). **TROYER, Deryl, L.** [US/US]; 5524 Anderson Ave., Manhattan, KS 66503 (US). **BASEL, Matthew, T.** [US/US]; 340 North 16th, Apartment 3, Manhattan, KS 66502 (US).

(74) Agent: **SKOCH, Gregory, J.**; Hovey Williams Llp, 10801 Mastin Blvd. Suite 1000, 84 Corporate Woods, Overland Park, KS 66210 (US).

(81) Designated States *(unless otherwise indicated, for every kind of national protection available)*: AE, AG, AL, AM, AO, AT, AU, AZ, BA, BB, BG, BH, BR, BW, BY, BZ, CA, CH, CN, CO, CR, CU, CZ, DE, DK, DM, DO, DZ, EC, EE, EG, ES, FI, GB, GD, GE, GH, GM, GT, HN, HR, HU, ID, IL, IN, IS, JP, KE, KG, KM, KN, KP, KR, KZ, LA, LC, LK, LR, LS, LT, LU, LY, MA, MD, ME, MG, MK, MN, MW, MX, MY, MZ, NA, NG, NI, NO, NZ, OM, PG, PH, PL, PT, RO, RS, RU, SC, SD, SE, SG, SK, SL, SM, ST, SV, SY, TJ, TM, TN, TR, TT, TZ, UA, UG, US, UZ, VC, VN, ZA, ZM, ZW.

(84) Designated States *(unless otherwise indicated, for every kind of regional protection available)*: ARIPO (BW, GH, GM, KE, LS, MW, MZ, NA, SD, SL, SZ, TZ, UG, ZM, ZW), Eurasian (AM, AZ, BY, KG, KZ, MD, RU, TJ, TM), European (AT, BE, BG, CH, CY, CZ, DE, DK, EE, ES, FI, FR, GB, GR, HR, HU, IE, IS, IT, LT, LU, LV, MC, MK, MT, NL, NO, PL, PT, RO, SE, SI, SK, TR), OAPI (BF, BJ, CF, CG, CI, CM, GA, GN, GQ, GW, ML, MR, NE, SN, TD, TG).

Published:

— *without international search report and to be republished upon receipt of that report (Rule 48.2(g))*

— *with sequence listing part of description (Rule 5.2(a))*

WO 2009/111470 A2

(54) Title: PROTEASE ASSAY

(57) Abstract: The present invention provides a diagnostic reagent or assay for assessing the activity of a protease in vivo or in vitro and methods of detecting the presence of a cancerous or precancerous cell. The assays are comprised of two particles linked via an oligopeptide linkage that comprises a consensus sequence specific for the target protease. Cleavage of the sequence by the target protease can be detected visually or using various sensors, and the diagnostic results can be correlated with cancer prognosis.

PROTEASE ASSAY

CROSS-REFERENCE TO RELATED APPLICATIONS

This application claims the priority benefit of a provisional application entitled FLUORESCENT PROTEASE ASSAY, Serial No. 61/067,891, filed March 3, 2008, incorporated by reference herein in its entirety.

SEQUENCE LISTING

The following application contains a sequence listing in computer readable format (CRF), submitted as a text file in ASCII format entitled "40132-PCT," created on February 25, 2009, as 9 KB. The contents of the CRF are hereby incorporated by reference.

BACKGROUND OF THE INVENTION

Field of the Invention

The present invention relates in general to diagnostic assays for detecting protease activity associated with cancer, correlation of diagnostic results with cancer prognosis, and methods of detecting the presence of a cancerous or precancerous cell.

Description of the Prior Art

Cancer prognosis is based upon the stage of the disease. The four major stages are initial mutations, cell survival and tumor progression, angiogenesis, and finally invasion or metastasis. One of the biggest challenges is that cancer is a disease of the body's own cells. Because of this, it is often very challenging to diagnose cancer until the disease is quite progressed. This also affects treatment efficiency, since the cancer cells have the same enzymes, replication equipment, structural features, etc. as healthy cells, treatments that delineate cancer cells from healthy cells are difficult to develop. This is why staging and treatment is usually based on the symptoms (i.e., the size of the tumor, whether lymph nodes contain cancer, and whether the cancer has spread from the original site to other parts of the body), rather than on specifically targeting the origin of the cancer.

More recently, a number of proteases have been associated with disease progression

in cancer. Proteases are a class of enzyme that catalyze the cleavage of the peptide bond in other proteins. They can be very specific (only being able to degrade one peptide bond in one protein) or extremely broad (e.g., being able to cleave the peptide bond every time there is, for example, a lysine). Several proteases are known to be over-expressed by various cancer cell lines. Proteases that are known to be necessary for cancer development and progression include Matrix Metalloproteinases (MMPs), Tissue Serine Proteases, and the Cathepsins. Many of these proteases are either upregulated in the cancer cells (that is, they have a much higher activity in the tumor than in healthy tissue), mis-expressed (that is, they are found in compartments where they should not be found), or are involved in embryonic development, but should not be found to any significant extent in an adult cells.

MMPs are the classic cancer-associated proteases. MMPs are a family of zinc proteases that are named for the zinc and calcium ions that are required as cofactors. There are 21 different known MMPs that are grouped into families based on their substrates: collagenases, gelatinases, stromelysins, matrilysin, metalloelastase, enamelysin, and membrane-type MMPs. As can be seen from the family names, MMPs degrade the proteins that make up the extracellular matrix (ECM) and the basement membrane (BM) of tissue. MMPs are usually not produced by the cancerous cells themselves, but by the stromal cells surrounding the tumor. This is because the cancerous cells give off a variety of cell signals that cause the surrounding stromal cells to highly upregulate their production of MMPs. MMPs are vital to cancer survival and progression for several reasons. First, they cleave cell surface bound growth factors from the stromal and epithelial cells and release them to interact with the cancer cells to stimulate growth. They also play a role in angiogenesis by opening the ECM to new vessel development as well as by releasing pro-angiogenic factors and starting pro-angiogenic protease cascades. MMPs play a major role in tumor metastasis by degrading the ECM and the BM, allowing the cells to pass through tissue barriers. They also release ECM and BM fragments, which stimulates cell movement.

Several serine proteases have well-documented roles in cancer as well, especially urokinase plasminogen activator (uPA) and plasmin. Elevated expression levels of urokinase and several other components of the plasminogen activation system have been found to be correlated with tumor malignancy. uPA is a very specific protease that binds

to its receptor, uPAR, and cleaves the inactive plasminogen (a zymogen) to the active plasmin. This is the first step in a well-known cascade that causes angiogenesis. It is believed that the tissue degradation that follows plasminogen activation facilitates tissue invasion and contributes to metastasis.

Cathepsins, with a few exceptions, are cysteine proteases. Often found in the lysosomal/endosomal pathway, cathepsins usually operate at low pH values, but some are still active at neutral pH. Three of the cathepsins, B, D, and L, are active at neutral pH and are often misexpressed in cancer, causing activation outside of the cells. This activation outside of the cell can cause ECM degradation.

Many studies directed to assess the prognostic impact of the plasminogen/plasmin components have been conducted, mostly based on antigen level quantitation in tissue extracts from surgically removed tumors. These values have been subsequently correlated with prognosis in several types of cancers. However, determining ways to distinguish cancerous cells from healthy cells remains a large area of research in cancer therapy, and there is still a need in the art for methods of quantitatively detecting cancer progression and stages of the disease that can be applied in vitro and in vivo. There is also a need for detecting multiple markers of the various cancer stages at one time without the need for separate tests. There also is a need for in vivo characterization of cancer, so that treatment can be directed to the most malignant cancer tissue.

SUMMARY OF THE INVENTION

The present invention provides a nanoplatform assembly for detecting protease activity comprising a first particle, a second particle, and a linkage between the first and second particles, wherein the linkage comprises a protease consensus sequence.

The invention also provides a composition comprising a diagnostic assay for assessing the activity of a protease and a pharmaceutically-acceptable carrier. The diagnostic assay includes the nanoplatform assembly comprising a first particle, a second particle, and a linkage between the first and second particles, wherein the linkage comprises a consensus sequence specific to the protease.

In addition, the invention provides a method for detecting the activity of a protease

associated with a cancerous or precancerous cell in a mammal. The method comprises contacting a fluid sample from the mammal with a diagnostic assay. The diagnostic assay comprises a nanoplatform assembly, the nanoplatform assembly comprising a first particle, a second particle, and a linkage between the first and second particles, wherein the linkage comprises a consensus sequence specific to the protease. The assay is exposed to an energy source to excite the assay. The changes in the absorption or emission spectrum of the assay are then detected. These changes correspond to protease activity.

The invention provides a further method for detecting the activity of a protease associated with a cancerous or precancerous cell in a mammal. The inventive method comprises administering to the mammal a composition comprising the inventive diagnostic assay for assessing the activity of a protease and a pharmaceutically-acceptable carrier. The assay in composition is then activated. The region of the mammal suspected of having a cancerous or precancerous cell is exposed to an energy source, which excites the assay, and the changes in the absorption or emission spectrum of the assay are detected. These changes correspond to protease activity, which can then be correlated with a prognosis for cancer progression.

BRIEF DESCRIPTION OF THE DRAWINGS

Figure 1 depicts the four main stages of cancer progression and the proteases associated with these stages;

Fig. 2 illustrates the spectral shift in the plasmon absorption of the coupled pair of gold nanoparticles before, during, and after urokinase cleavage of the oligopeptide in Example 3;

Fig. 3 illustrates the emission spectra of the nanoplatform assembly in Example 4;

Fig. 4 illustrates the emission spectra of the nanoplatform assembly and FRET-based sensor from Example 5;

Fig. 5 depicts the ratios of the integrals of the fluorescence bands shown at λ_1= 607 nm, λ_2= 654 nm, and λ_3= 718 nm plotted versus the mol percent of released TCPP in Example 5;

Fig. 6 illustrates the data from the assay in urine from rats impregnated with MATB III type cancer cells using the light switch-based sensor in Example 5;

Fig. 7 shows the plot of the relative intensities of the luminescence of TCPP occurring at λ=656 nm using the data from Figure 6;

Fig. 8 shows the plot of the relative intensities of the luminescence of TCPP occurring at λ=656 nm when measuring urine of rats, which have been impregnated with MATBIII cells 15 days prior to sampling the urine in Example 5;

Fig. 9 shows the plot of the relative intensities of the luminescence of TCPP occurring at λ=656 nm when measuring urine of rats, which have been impregnated with MATBIII cells 5 days prior to sampling the urine in Example 5;

Fig. 10 illustrates the growth of CdSe quantum dots during synthesis as indicated by their luminescence from Example 6. The inset shows a representative image of a highly crystalline CdSe quantum dot with wurzit structure;

Fig. 11 illustrates the single-photo-counting spectra, from the right and left limbs of the mice from Example 7, recorded through a fluorescence microscope; and

Fig. 12 illustrates the calibration curve results from Example 8.

DETAILED DESCRIPTION OF THE PREFERRED EMBODIMENTS

It has been found that the presence of certain proteases can serve as a marker for the ability of many cancers to grow and eventually metastasize. The present invention provides diagnostic assays and methods of detecting protease activity and diagnosing corresponding disease progression. The inventive assays can be used to detect any protease or enzyme that cleaves a DNA-, RNA-, carbohydrate-, or protein-based linker.

The diagnostic assays of the invention comprise a nanoplatform assembly. The nanoplatform assembly is comprised of a protease consensus sequence (the sequence of amino acids cleaved by the protease), which is used as a linker between two particles. More preferably, the linker is comprised of an oligopeptide containing the consensus sequence.

Oligopeptide Linkages and Consensus Sequences

Suitable oligopeptides will comprise a terminal carboxylic acid group (C terminus) and a terminal amine group (N terminus). The oligopeptide also preferably comprises a

thiol group at the C terminus, although this may be modified depending upon the particles used in the nanoplatform assembly. More preferably, the oligopeptide linker comprises a hydrophilic region of at least 10 amino acids N-terminal to the protease consensus sequence, and a linking region C-terminal to the cleavage sequence, wherein the C-terminal linking region comprises a thiol reactive group at its terminus. Even more preferably, the C terminus of the oligopeptide comprises a cysteine residue, lysine, or aspartate. The N-terminal hydrophilic region of the oligopeptide preferably has an excess positive or negative charge at a ratio of about 1:1. The N-terminal hydrophilic region also preferably comprises amino acid residues capable of forming hydrogen bonds with each other.

Particularly preferred C-terminal linking regions comprise a sequence selected from the group consisting of GGGC (SEQ ID NO: 14), AAAC (SEQ ID NO: 15), SSSC (SEQ ID NO: 16), TTTC (SEQ ID NO: 17), GGC (SEQ ID NO: 38), GGK (SEQ ID NO: 39), GC (SEQ ID NO: 40), and GGD (SEQ ID NO: 42). Particularly preferred N-terminal regions of the oligopeptide comprise a sequence selected from the group consisting of SRSRSRSRSR (SEQ ID NO: 1), KSRSRSRSRSR (SEQ ID NO: 19), KKSRSRSRSRSR (SEQ ID NO: 20), CGGG (SEQ ID NO: 23), KGGG (SEQ ID NO: 24), and KGG (SEQ ID NO: 37). The N-terminus preferably further comprises at least one terminal group selected from the group consisting of lysine, ornithine, 2,4 diaminobutyric acid, and 2,3 diaminoproprionic acid. Another preferred oligopeptide has the following general structure:

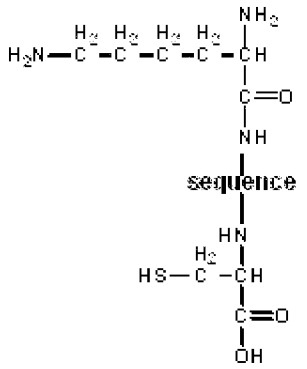

where the "sequence" can be any of the oligopeptide or consensus sequences described herein. The oligopeptides can be purchased, or they can be synthesized using known methods (e.g., modified Merrifield synthesis).

Preferably, the consensus sequence used in the inventive diagnostic assays is selected from the group consisting of serine protease cleavage sequences, aspartyl protease cleavage sequences, cysteine protease cleavage sequences, and metalloprotease cleaveage sequences. Even more preferably, the consensus sequence comprises a cleavage sequence for a protease selected from the group consisting of urokinase, matrix metallopeptidase, cathepsin, and gelatinase. Particularly preferred proteases and their corresponding consensus sequences are listed in Table I below.

Table I

Protease	**Consensus Sequence (Cleavage Sequence)**
MMP-1	VPMSMRGG (SEQ ID NO: 3)
MMP-2	IPVSLRSG (SEQ ID NO: 4)
MMP-3	RPFSMIMG (SEQ ID NO: 5)
MMP-7	VPLSLTMG (SEQ ID NO: 6)
MMP-9	VPLSLYSG (SEQ ID NO: 7)
MMP-11	HGPEGLRVGFYESDVMGRGHARLVHVEEPHT (SEQ ID NO: 25)
MMP-13	GPQGLAGQRGIV (SEQ ID NO: 26)
MT1-MMP	IPESLRAG (SEQ ID NO: 8)
uPA	SGRSA (SEQ ID NO: 2)
Cathepsin B	SLLKSRMVPNFN (SEQ ID NO: 27) DAFK (SEQ ID NO: 10)
Cathepsin D	SLLIFRSWANFN (SEQ ID NO: 28) SGKPILFFRL (SEQ ID NO: 11)
Cathepsin E	SGSPAFLAKNR (SEQ ID NO: 9) SGKPIIFFRL (SEQ ID NO: 12)
Cathepsin L	SGVVIATVIVIT (SEQ ID NO: 29)
Gelatinase	GPLGMLSQ (SEQ ID NO: 13)

With reference to Figure 1, the foregoing proteases are associated with many specific events in cancer progression. The stages of disease progression are separated into four events: initial mutation, cell survival/tumor progression, angiogenesis (development of new blood vessels), and invasion/tissue remodeling. The array of proteases associated with each stage can give a good picture of how far the cancer has progressed and what the prognosis will be. The preferred diagnostic reagents or assays comprise a protease consensus sequence for a protease selected from the group consisting of uPA, MMP-1, MMP-2, and MMP-7. The most preferred oligopeptide sequences for detecting uPA,

MMP-1, MMP-2, and MMP-7, respectively, are listed in the table below with the point of cleavage indicated by "-".

Table II

Protease	Preferred Oligopeptide with Consensus Sequence
MMP-1	KGG**VPMS-MRGG**GC (SEQ ID NO: 30)
MMP-2	KGG**IPVS-LRSG**GC (SEQ ID NO: 31)
MMP-7	KGG**VPLS-LTMG**GC (SEQ ID NO: 32)
uPA	KGGG**SGR-SA**GGGC (SEQ ID NO: 33) CGGG**SGR-SA**GGC (SEQ ID NO: 34) CGGG**SGR-SA**GGGC (SEQ ID NO: 35) DGG**SGR-SA**GGK (SEQ ID NO: 36) SRSRSRSRSR**SGR-SA**GGGC (SEQ ID NO: 18) KGG**SGR-SA**GGD (SEQ ID NO: 41)

With reference again to Figure 1, an accurate cancer prognosis can be determined using the inventive assays. In particular, if MMP-1 and MMP-7, but neither of the other two proteases are detected by the inventive assays, the cancer prognosis is for cell survival/tumor progression. If uPA and MMP-7 are detected by the assays (but not MMP-1 or MMP-2), the prognosis is for angiogenesis. If all four proteases are detected, the prognosis is for invasion and eventual metastasis. Thus, the in-vivo measurements of these four proteases enable the spatially resolved determination of the progression of cancerous tissue, and permit a more detailed prognosis that can guide the treatment towards the most active tumors in the body.

In the presence of the protease, the consensus sequence of the nanoplatform assembly is cleaved, and the spectral change caused by this cleavage is detected by the inventive assays. Thus, depending upon the proteases targeted by the nanoplatform, two or more of the following sequences will result: KGGVPMS (SEQ ID NO: 43), MRGGGC (SEQ ID NO: 44), KGGIPVS (SEQ ID NO: 45), LRSGGC (SEQ ID NO: 46), KGGVPLS (SEQ ID NO: 47), LTMGGC (SEQ ID NO: 48), KGGGSGR (SEQ ID NO: 49), SAGGGC (SEQ ID NO: 50), CGGGSGR (SEQ ID NO: 51), SAGGC (SEQ ID NO: 52), DGGSGR (SEQ ID NO: 53), SAGGK (SEQ ID NO: 54), SRSRSRSRSRSGR (SEQ ID NO: 55), KGGSGR (SEQ ID NO: 56), or SAGGD (SEQ ID NO: 57).

Particles for Assay

A number of different types of particles can be used to form the nanoplatform assemblies for use in the inventive assays, depending upon the type of sensor used to measure the protease activity, as discussed in more detail below. Preferably, the excitation and emission spectral maxima of the particles are between 650 and 800 nm. Preferred particles for use in the diagnostic assays are selected from the group consisting of nanoparticles (e.g., metal, metal alloy, or core/shell), chromophores/luminophores, quantum dots, viologens, and combinations thereof.

1. Nanoparticles

The term "nanoparticle" as used herein refers to metal nanocrystalline particles that can optionally be surrounded by a metal or nonmetal nanolayer shell. Suitable nanoparticles preferably have a diameter of from about 1 nm to about 100 nm, more preferably from about 10 nm to about 50 nm, and even more preferably from about 5 nm to about 20 nm. The nanoparticles can comprise any type of metal (including elemental metal) or metal alloy. Preferably, the metal or metal alloy nanoparticles comprise a metal selected from the group consisting of gold (Au), silver (Ag), copper (Cu), nickel (Ni), palladium (Pd), platinum (Pt), cobalt (Co), rhodium (Rh), iridium (Ir), iron (Fe), ruthenium (Ru), osmium (Os), manganese (Mn), rhenium (Re), scandium (Sc), titanium (Ti), vanadium (V), chromium (Cr), zinc (Zn), yttrium (Y), zirconium (Zr), niobium (Nb), molybdenum (Mo), technetium (Tc), cadmium (Cd), lanthanum (La), lutetium (Lu), hafnium (Hf), tantalum (Ta), tungsten (W), actinium (Ac), lawrencium (Lr), rutherfordium (Rf), dubnium (Db), seaborgium (Sg), bohrium (Bh), Hassium (Hs), meitnerium (Mt), darmstadtium (Ds), roentgenium (Rg), ununbium (Uub), selenium (Se), and the oxides (e.g., FeO, Fe_3O_4, Fe_2O_3, Fe_xO_y (non-stoichiometric iron oxide), CuO, NiO, Ag_2O, Mn_2O_3), hydroxides, sulfides, selenides, and tellurides of the foregoing, and combinations thereof.

Core/shell nanoparticles preferably comprise a metal or metal alloy core and a metal shell. Preferred cores are selected from the group consisting of Au, Ag, Cu, Co, Fe, and Pt. Preferred shells are selected from the group consisting of Au, Ag, Cu, Co, Fe, Pt, the metal oxides thereof, and combinations thereof. Particularly preferred metal core/shell

combinations are selected from the group consisting of Fe/Au, Fe/Fe_3O_4, and Au/Fe_2O_3. The core of the nanoparticle preferably has a diameter of from about 1 nm to about 25 nm, and more preferably from about 3 nm to about 5 nm. The metal shell of the core/shell nanoparticle preferably has a thickness of from about 0.5 nm to about 10 nm, and more preferably from about 0.5 to about 2 nm.

The nanoparticles can be stabilized or non-stabilized. Stabilized nanoparticles preferably comprise an organic monolayer surrounding the nanoparticle core. The term "stabilized" as used herein means the use of a ligand shell or monolayer to coat, protect (e.g., from bio-corrosion), or impart properties (e.g., water solubility) to, the nanoparticle. The monolayer can be comprised of several of the same ligands (i.e., homoligand) or of mixed ligands. Various techniques for attaching ligands to the surface of various nanoparticles are known in the art. For example, nanoparticles may be mixed in a solution containing the ligands to promote the coating of the nanoparticle. Alternatively, coatings may be applied to nanoparticles by exposing the nanoparticles to a vapor phase of the coating material such that the coating attaches to or bonds with the nanoparticle. Preferably, the ligands attach to the nanoparticle through covalent bonding. The number of ligands required to form a monolayer will be dependent upon the size of the nanoparticle.

The ligands comprise functional groups that are attracted to the nanoparticle's metal surface. Preferably, the ligands comprise at least one group selected from the group consisting of thiols, alcohols, nitro compounds, phosphines, phosphine oxides, resorcinarenes, selenides, phosphinic acids, phosphonicacids, sulfonic acids, sulfonates, carboxylic acids, disulfides, peroxides, amines, nitriles, isonitriles, thionitiles, oxynitriles, oxysilanes, alkanes, alkenes, alkynes, aromatic compounds, and seleno moieties. Preferred organic monolayers are selected from the group consisting of alkanethiolate monolayers, aminoalkylthiolate monolayers, alkylthiolsulfate monolayers, and organic phenols (e.g., dopamine and derivatives thereof). The thickness of the organic monolayer is preferably less than about 10 nm, and more preferably less than about 5 nm. Particularly preferred stabilized nanoparticles are selected from the group consisting of trioctyl-phosphinoxide-stablized nanoparticles, amine-stabilized nanoparticles, carboxylic-acid-stabilized nanoparticles, phosphine-stabilized nanoparticles,

thiol-stabilized nanoparticles, aminoalkylthiol-stabilized nanoparticles, and organic phenol-stabilized nanoparticles.

2. *Chromophores/Luminophores*

Chromophore/luminophore particles suitable for use in the inventive assays include any organic or inorganic dyes, fluorophores, phosphophores, light absorbing nanoparticles (e.g., Au, Ag, Pt, Pd), combinations thereof, or the metalated complexes thereof. Preferably, the chromophore/luminophore particles have a size of less than about 100 nm.

Suitable organic dyes are selected from the group consisting of coumarins, pyrene, cyanines, benzenes, N-methylcarbazole, erythrosin B, N-acetyl-L-tryptophanamide, 2,5-diphenyloxazole, rubrene, and N-(3-sulfopropyl)acridinium. Specific examples of preferred coumarins include 7-aminocoumarin, 7-dialkylamino coumarin, and coumarin 153. Examples of preferred benzenes include 1,4-bis(5-phenyloxazol-2-yl)benzene and 1,4-diphenylbenzene. Examples of preferred cyanines include oxacyanines, thiacyanines, indocyanins, merocyanines, and carbocyanines. Other exemplary cyanines include ECL Plus, ECF, C3-Oxacyanine, C3-Thiacyanine Dye (EtOH), C3-Thiacyanine Dye (PrOH), C5-Indocyanine, C5-Oxacyanine, C5-Thiacyanine, C7-Indocyanine, C7-Oxacyanine, CypHer5, Dye-33, Cy7, Cy5, Cy5.5, Cy3Cy5 ET, Cy3B, Cy3, Cy3.5, Cy2, CBQCA, NIR1, NIR2, NIR3, NIR4, NIR820, SNIR1, SNIR2, SNIR4, Merocyanine 540, Pinacyanol-Iodide, 1,1-Diethyl-4,4-carbocyanine iodide, Stains All, Dye-1041, or Dye-304.

Suitable inorganic dyes are selected from the group consisting of metalated and non-metalated porphyrins, phthalocyanines, chlorins (e.g., chlorophyll A and B), and metalated chromophores. Preferred porphyrins are selected from the group consisting of tetra carboxy-phenyl-porphyrin (TCPP) and Zn-TCPP. Preferred metalated chromophores are selected from the group consisting of ruthenium polypyridyl complexes, osmium polypyridyl complexes, rhodium polypyridyl complexes, 3-(1-methylbenzoimidazol-2-yl)-7-(diethylamino)-coumarin complexes of iridium(III), and 3-(benzothiazol-2-yl)-7-(diethylamino)-coumarin complexes with iridium(III).

Suitable fluorophores and phosphophores are selected from the group consisting of phosphorescent dyes, fluoresceines, rhodamines (e.g., rhodamine B, rhodamine 6G),

and anthracenes (e.g., 9-cyanoanthracene, 9,10-diphenylanthracene, 1-Chloro-9,10-bis(phenylethynyl)anthracene).

3. Quantum Dots

A quantum dot is a semiconductor composed of atoms from groups II-VI or III-V elements of the periodic table (e.g., CdSe. CdTe, InP). The optical properties of quantum dots can be manipulated by synthesizing a (usually stabilizing) shell. Such quantum dots are known as core-shell quantum dots (e.g., CdSe/ZnS, InP/ZnS, InP/CdSe). Quantum dots of the same material, but with different sizes, can emit light of different colors. Their brightness is attributed to the quantization of energy levels due to confinement of an electron in all three spatial dimensions. In a bulk semiconductor, an electron-hole pair is bound within the Bohr exciton radius, which is characteristic for each type of semiconductor. A quantum dot is smaller than the Bohr exciton radius, which causes the appearance of discrete energy levels. The band gap, ΔE, between the valance and conduction band of the semiconductor is a function of the nanocrystal's size and shape. Quantum dots feature slightly lower luminescence quantum yields than traditional organic fluorophores but they have much larger absorption cross-sections and very low rates of photobleaching. Molar extinction coefficients of quantum dots are about 10^5 - 10^6 M^{-1} cm^{-1}, which is 10-100 times larger than dyes.

Core/shell quantum dots have higher band gap shells around their lower band gap cores, which emit light without any absorption by the shell. The shell passivates surface nonradiative emission from the core thereby enhancing the photoluminescence quantum yield and preventing natural degradation. The shell of type I quantum dots (e.g. CdSe/ZnS) has a higher energy conduction band and a lower energy valance band than that of the core, resulting in confinement of both electron and hole in the core. The conduction and valance bands of the shell of type II quantum dots (e.g., CdTe/CdSe, CdSe/ZnTe) are either both lower or both higher in energy than those of the core. Thus, the motions of the electron and the hole are restricted to one dimension. Radiative recombination of the exciton at the core-shell interface gives rise to the type-II emission. Type II quantum dots behave as indirect semiconductors near band edges and therefore, have an absorption tail into the red and near infrared. Alloyed semiconductor quantum dots (CdSeTe) can also be used,

although types I and II are most preferred. The alloy composition and internal structure, which can be varied, permits tuning the optical properties without changing the particles' size. These quantum dots can be used to develop near infrared fluorescent probes for in vivo biological assays as they can emit up to 850 nm.

Particularly preferred quantum dots are selected from the group consisting of CdSe/ZnS core/shell quantum dots, CdTe/CdSe core/shell quantum dots, CdSe/ZnTe core/shell quantum dots, and alloyed semiconductor quantum dots (e.g., CdSeTe). The quantum dots are preferably small enough to be discharged via the renal pathway when used in vivo. More preferably, the quantum dots are less than about 10 nm in diameter, even more preferably from about 2 nm to about 5.5 nm in diameter, and most preferably from about 1.5 nm to about 4.5 nm in diameter. If different color emission is needed for creating multiple sensors (multiplex detection), this can be achieved by changing the size of the quantum dot core yielding different emission wavelengths. The quantum dots can be stabilized or unstabilized as discussed above regarding nanoparticles. Preferred ligands for stabilizing quantum dots are resorcinarenes.

Nanoplatform Assemblies for Assays

The diagnostic nanoplatform assemblies comprise at least two particles linked together via the oligopeptide sequences discussed above. In addition, the assemblies can comprise multiple particles linked to a single central particle, depending upon the particles used and the spectrum used to detect the assay. If the whole visible and near IR spectrum are used during detection, up to ten particles can be linked to a central particle (for detecting up to 10 different proteases in a single assay, if different cleavage sequences are used to link each particle). If either the visible spectrum or IR spectrum is used alone, up to five particles can be linked to a central particle (for detecting up to 5 different proteases in a single assay, if different cleavage sequences are used to link each particle). The linkage between the particles, in addition to the oligopeptide sequence, can be further comprised of ligands or spacer moieties (discussed below) attached to either particle.

The assemblies can be comprised of the same type of particles (i.e., a nanoparticle linked to a nanoparticle), or of different particles (i.e., a nanoparticle linked to a different type of particle, such as a chromophore/luminophore or quantum dot). The assemblies can

also be comprised of a chromophore/luminophore linked to a chromophore/luminophore. When two nanoparticles are used in the same diagnostic assembly, they can be identical (i.e., comprise the same kind of metal, alloy, or core/shell, and be the same shape (e.g., round, globular, rod-shaped, etc.)), or each particle can be different (i.e., non-identical, physically and/or chemically). Preferably, the particles have different chemical compositions and sizes, and the assemblies are created using different nanoparticles or chromophores/luminophores, or the assembly is created between a nanoparticle and a chromophore/luminophores (i.e., non-identical particles). In one aspect, the assemblies comprise two fluorophores separated by a distance that enables fluorescence resonance energy transfer or surface plasmon resonance between the two fluorophores. Each fluorophore comprises a fluorescent nanoparticle or a fluorescent organic dye, and are each bonded to a respective terminus of the oligopeptide linker that comprises the protease cleavage sequence.

The distance between the particles in the assembly will be dependent upon the length of the oligopeptide linker, as well as any ligands or spacers attached to either particle. However, the distance is preferably less than about 10 nm, more preferably less than about 5 nm, and even more preferably from about 1 nm to about 3 nm.

In the case of chromophores/luminophores, such particles are preferably covalently bonded to the oligopeptide linker, optionally, via a spacer moiety bound to the chromophore/luminophore. Depending upon which end of the oligopeptide the spacer will be linked to, preferred spacer moieties comprise reactive groups selected from the group consisting of carboxyls, thiols, and combinations thereof. In one preferred embodiment, the spacer moiety is covalently attached to the N-terminus of the oligopeptide linker through an amide bond. In an alternative embodiment, the spacer moiety is covalently attached to the C-terminus of the oligopeptide linker through a disulfide bond. Particularly preferred spacer moieties include ethylene glycols (preferably C_3-C_{20}, such as tetraethylene glycols to dodecaethylene glycols), amides (preferably C_3-C_{20}), alkylenes (preferably C_3-C_{20}), or esters (preferably C_3-C_{20}), each having two terminal carboxyl groups or a terminal carboxyl group and a terminal thiol group.

The diagnostic assays can be utilized as is, or can be part of a composition comprising the diagnostic assay and a pharmaceutically-acceptable carrier. For in vivo

diagnostics, the assays will preferably be delivered using a pharmaceutically-acceptable carrier. A suitable example includes traditional liposomal delivery, discussed in more detail below.

The assays can be used to detect cancerous or pre-cancerous cells associated with a cancer selected from the group consisting of an AIDS-related cancer, AIDS-related lymphoma, anal cancer, appendix cancer, childhood cerebellar astrocytoma, childhood cerebral astrocytoma, basal cell carcinoma, extrahepatic bile duct cancer, childhood brain stem glioma, adult brain tumor, childhood malignant glioma, childhood ependymoma, childhood medulloblastoma, childhood supratentorial primitive neuroectodermal tumors, childhood visual pathway and hypothalamic glioma, breast cancer, pregnancy-related breast cancer, childhood breast cancer, male breast cancer, childhood carcinoid tumor, gastrointestinal carcinoid tumor, primary central nervous system lymphoma, cervical cancer, colon cancer, childhood colorectal cancer, esophageal cancer, childhood esophageal cancer, intraocular melanoma, retinoblastoma, adult glioma, adult (primary) hepatocellular cancer, childhood (primary) hepatocellular cancer, adult Hodgkin lymphoma, childhood Hodgkin lymphoma, islet cell tumors, Kaposi Sarcoma, kidney (renal cell) cancer, childhood kidney cancer, adult (primary) liver cancer, childhood (primary) liver cancer, Non-small cell liver cancer, small cell liver cancer, AIDS-related lymphoma, Burkitt lymphoma, adult Non-Hodgkin lymphoma, childhood Non-Hodgkin lymphoma, primary central nervous system lymphoma, melanoma, adult malignant mesothelioma, childhood mesothelioma, metastatic squamous neck cancer with occult primary, mouth cancer, childhood multiple endocrine neoplasia syndrome, multiple myeloma/plasma cell neoplasm, mycosis fungoides, myelodysplastic syndromes, myelodysplastic/myeloproliferative diseases, adult acute myeloid leukemia, childhood acute myeloid leukemia, multiple myeloma, neuroblastoma, non-small cell lung cancer, childhood ovarian cancer, ovarian epithelial cancer, ovarian germ cell tumor, ovarian low malignant potential tumor, pancreatic cancer, childhood pancreatic cancer, islet cell pancreatic cancer, parathyroid cancer, penile cancer, plasma cell neoplasm/multiple myeloma, pleuropulmonary blastoma, prostate cancer, rectal cancer, childhood renal cell cancer, renal pelvis and ureter, transitional cell cancer, adult soft tissue sarcoma, childhood soft tissue sarcoma, uterine sarcoma, skin cancer (nonmelanoma), childhood skin cancer,

melanoma, Merkel cell skin carcinoma, small cell lung cancer, small intestine cancer, squamous cell carcinoma, stomach cancer, childhood stomach cancer, cutaneous T-Cell lymphoma, testicular cancer, thyroid cancer, childhood thyroid cancer, and vaginal cancer.

The Inventive Methods

One advantage of the inventive assays is the flexibility to adapt the assays by modifying the particles to suit the sensor technology available, and likewise, using a variety of sensor technologies for detecting enzyme activity depending upon the particles available.

1. FRET-Based Sensors

In one aspect of the invention, the assays work on the basis of surface plasmon resonance and Förster resonance energy transfer (FRET) between non-identical particles, such as particles having different chemical compositions or sizes, or between different chromophores/luminophores, or between a nanoparticle and a chromophore/luminophore, linked by the cleavage sequences. FRET describes energy transfer between two particles. Surface plasmon resonance is used to excite the particles. A donor particle initially in its excited state, may transfer this energy to an acceptor particle in close proximity through nonradiative dipole-dipole coupling. When both particles are fluorescent chromophores/luminophores, the term "fluorescence resonance energy transfer" is often used instead, although the energy is not actually transferred by fluorescence. In the present invention, FRET is used to detect protease cleavage. Briefly, while the particles are bound by the oligopeptide, emission from the acceptor is observed upon excitation of the donor particle. Once the enzyme cleaves the linkage between the particles, FRET change is observed, and the emission spectra changes. Only the donor emission is observed.

In more detail, if both particles are within the so-called Förster-distance, energy transfer occurs between the two particles and a red-shift in absorbance and emission is observed. During this ultrafast process, the energy of the electronically excited state or surface plasmon of the first particle is at least partially transferred to the second particle. Under these conditions, light is emitted from the second particle. However, once the bond between the two particles is cleaved by the enzyme, light is emitted only from the first

particle and a distinct blue-shift in absorption and emission is observed. This is because the distance between both particles greatly increases (see equation below).

The maximum of the observed plasmon resonance can be characterized by the following equation.

$$\frac{\Delta\lambda}{\lambda_0} \approx c \exp \frac{-(s / D)}{d}$$

where $\Delta\lambda/\lambda_0$ is the fractional plasmon shift, c and d are constants, s is the edge-to-edge distance between the particles, and D is the particle diameter. In the nanoplatform assemblies the distance separating the particles can be calculated to be about 0.3 nm per amino acid present in the oligopeptide. The FRET efficiency ("E") can be characterized as

$$E = \frac{1}{1 + \left(\frac{R}{R_0}\right)^6}$$

where R_0 is the Förster distance (i.e., the distance at which the donor transfers 50% of its energy to the acceptor via FRET). Both particles for use with the FRET assays can be chosen so that the absorption and emission wavelengths of each particle are distinctly different, and will therefore appear as distinct luminescent bands. Preferably, the assays can be performed in vitro and in vivo. Therefore, excitation of the first particle can preferably performed between about 400 nm and about 1000 nm, more preferably between about 500 nm to about 800 nm, and even more preferably between about 650 nm and about 800 nm in order to minimize absorption and scattering by human tissue for in vivo use. When using chromophore/luminophore particles, there is also preferably an overlap between the excitation spectrum of the first chromophore/luminophore and the fluorescence or phosphorescence spectrum of the second chromophore/luminophore to permit adequate Förster energy transfer.

a. In vitro methods

The assays may be used to detect protease activity in a fluid sample comprising a biological fluid, such as urine or blood samples of a mammal. In one aspect, a urine sample is collected from the mammal and physically mixed with the assay. Preferably, the concentration of the assay in the urine is from about $1x10^{-4}$M to about $1x10^{-10}$M, and more preferably from about $1x10^{-5}$M to about $1x10^{-8}$M. Excitation is preferably performed with an energy source of appropriate wavelength selected from the group consisting of a tungsten lamp, laser diode, laser, and bioluminescence (e.g., luciferase, renilla, green fluorescent protein). The wavelength used will depend upon the particles used in the nanoplatform assembly. Preferably, the wavelength ranges between about 400 nm and about 1000 nm, and more preferably between about 500 nm and 800 nm. The changes in absorption and emission of the particles as the protease in the urine sample cleaves the oligopeptide linkers will be observed over a time period of from about 1 second to about 30 minutes, and preferably from about 30 seconds to about 10 minutes, when in the presence of an aggressive tumor. In the presence of the protease, a typical absorption and emission blue-shift of between about 5 and about 200 nm will be observed. Thus, in the inventive method, a blue-shift in absorption or emission spectrum maximum between 5 and 200 nm preferably indicates the presence of a cancerous or precancerous cell in the mammal.

Blood can be collected from the mammal and analyzed like urine discussed above. Preferably, the concentration of the assay in the blood sample is from about $1x10^{-4}$ M to about $1x10^{-10}$ M, and more preferably from about $1x10^{-5}$ M to about $1x10^{-8}$ M. The wavelength used will depend upon the particles used in the nanoplatform assembly. Preferably, the wavelength ranges between about 500 nm and about 1000 nm, and more preferably between about 600 nm and 800 nm. More preferably, excitation is performed using multi-photon excitation at a wavelength of about 800 nm with a Ti-sapphire-laser because of the strong self-absorption of blood. Changes in emission will be observed over a time period of from about 1 second to about 30 minutes, and preferably from about 30 seconds to about 10 minutes, when in the presence of an aggressive tumor. As with urine, in the presence of the protease in the blood, a typical emission blue-shift of between about

5 and about 200 nm will be observed. This preferably indicates the presence of a cancerous or precancerous cell in the mammal.

These assay results (from urine or blood) can then be correlated with a prognosis for cancer progression, based upon the specific protease activity detected, as discussed above with regard to the preferred proteases, uPA, MMP-1, MMP-2, and MMP-7, or based upon the speed of the assay, as discussed below.

b. In vivo methods

In an alternative embodiment, detection of protease activity using the assays may be done in vivo in a mammal. The diagnostic assay, or composition comprising the assay, is preferably administered using a pharmaceutically-acceptable carrier. The assay can be administered by injection into the bloodstream. Alternatively, the assay can be administered by injection to a localized region, such as directly into or near the tumor site.

Delivery to the tumor site for in vivo analysis can be achieved by using liposomes (liposomal delivery). A liposome has a phospholipid bilayer and is preferably stabilized by the addition of cholesterol. Depending on the preparation method, liposome sizes range between 100 nm and several micrometers (preferably from about 100 nm to about 5 μm). Methods of preparing liposomes are known in the art. For example, the liposomes are preferably prepared by dissolving the phospholipids and the assay in a non-aqueous solvent such as chloroform ($CHCl_3$) or tetrahydrofuran (THF) in a reaction vessel (e.g., flask). This solvent is then evaporated using a rotovapor or other distillation device, which results in deposition of a film on the wall of the reaction vessel. A sucrose-solution in water (or any other sugar or salt combination) is then added to the vessel, followed by either freeze-thaw cycles or sonication. The resulting slurry is then preferably extruded through nanoporous filters to form mono-walled liposomes which are more preferred delivery agents.

The liposome containing the assay is then preferably injected into the bloodstream. Advantageously, when injected into the bloodstream, liposomes cannot exit the blood vessels, except in the vicinity of tumors, where blood vessels are "leaky" because of the rapid tumor growth. Therefore, the liposomes preferably become enriched in the vicinity of tumors (i.e., passive targeting). This process can be enhanced by chemically attaching

tumor-specific antibodies or aptamers to the liposomes (i.e., active targeting) according to known methods. The liposomes are then preferably destabilized while in the interstitium between the cancer cells to release the assay and detect protease activity in this vicinity.

More preferably, thermolabile liposomes are used. Thermolabile liposomes contain a polymer of the N-isopropyl-acrylamide type (e.g., a poly(NIPAM/ethylene glycol) block-copolymer), which can be anchored in the phospholipid bilayer of the liposomes via chemically attached long-chain-fatty acids or -alcohols. The liposome can then be heated once it reaches the target site by means of photophysical irradiation at 800 nm using at least two intersecting Ti:sapphire lasers. Preferably, the liposome is heated to a temperature to at least about 38°C, and more preferably at least about 45°C. This will cause the thermocollapse of the thermosensitive liposomes.

Photophysical heating (e.g., plasmonic heating, if nanoparticles are involved) will heat the nanoparticles of the assay, which then will dissipate the heat to the liposomes. That is, when metal nanoparticles are placed in an oscillating electric field, the 'free' electrons will respond to the periodic perturbation. Once the driving electric field is turned off, the oscillation of free electrons rapidly decays on a timescale of a few ps, with the acquired energy ultimately given off as heat due to participation by various scattering processes (i.e. electron-electron, electron-phonon, phonon-surface, etc.). Fast relaxation ensures that heat can be generated repeatedly, and large quantities of energy can be deposited into the nanoparticles. When metal nanoparticles are placed in a solvent bath, this method of heating can lead to a heat source, which is not in thermal equilibrium with its surroundings.

As mentioned, in an alternative embodiment for in-vivo imaging, the assay, dissolved in an aqueous buffer (e.g., phosphate buffered saline (PBS)), can be directly injected into the tumor or tumor-region. In the case of brain tumors, this may be the only viable option.

Once the assay is in the vicinity of the cancerous cells, one or two intersecting Ti:sapphire lasers are preferably used to excite the assay. Other suitable excitation sources include Nd:YAG-lasers (first harmonic at 1064 nm), and any kind of dye-laser, powered by the second harmonic of the Nd:YAG-laser at 532 nm. The light emission from the assay will then be analyzed using a camera, microscope, or confocal microscope. The light

emitted from the cancerous regions has a different color than the light emitted from the healthy tissue regions due to the higher activity of the target proteases in the cancerous regions. Advantageously, the cancerous tissue is then visibly discernible to an oncologist or surgeon, for example. Preferably, the Ti:sapphire laser is tuned to a wavelength of about 830 nm for the multi-photon excitation so that only the light emission, but not the excitation can be observed. The assay results can then be correlated with a prognosis for cancer progression, based upon the protease activity detected, as discussed in more detail below.

2. *Light-Switch-Based Sensors*

In another aspect, the assays utilize a nanoparticle linked by the oligopeptide-cleavage sequence to chromophores/luminophores or quantum dots. More than one chromophore/luminophore or quantum dot may be linked to a single central nanoparticle. However, when multiple particles are utilized, they preferably all comprise the same type of particle. Two preferred assemblies comprise at least one porphryin linked to a nanoparticle or at least one quantum dot linked to a nanoparticle. In this method, the surface plasmon of the core/shell nanoparticle is able to quench the excited state emission spectra from linked porphyrin. Likewise, quantum dots are highly luminescent, except when quenched by the presence of a core/shell metal nanoparticle. Viologens (e.g., methylviologen or propyl viologen-sulfonate (PVS)) can also be used as quenchers.

Once the protease cleaves the consensus sequence, the quantum dot or porphyrin is released and lights up, referred to herein as an "enzyme-triggered light switch." Advantageously, the appearance of a new luminescence/fluorescence band allows for much more sensitive detection. The emission wavelengths of quantum dots depend on their size, and assemblies can be constructed using one color (blue, green, yellow, red) of quantum dot assigned to each target enzyme. Up to four different consensus sequences can be linked to a single nanoparticle (one for each of the colors above). In this manner, the activity of up to four enzymes can be observed *in vivo* or *in vitro* at the same time. Preferably, excitation is performed at a wavelength of from about 400 nm to about 500 nm (monophotonic) or from about 800 nm to about 900 nm (multi-photonic). Excitation of the quantum dots can be performed by means of using low intensity visible photon sources,

or using ultrafast IR laser pulses. Other suitable excitation sources include Nd:YAG-lasers (first harmonic at 1064 nm), and any kind of dye-laser, powered by the second harmonic of the Nd:YAG-laser at 532 nm. Excitation of porphyrins is preferably performed using tri-photonic excitation with Ti:sapphire laser at 870 nm. The emission from the assay will then be analyzed using a camera, microscope, or confocal microscope. The light-switch-based sensors can be utilized in the exact same procedure (in vitro or in vivo) as the discussed above with regard to the FRET-based sensors.

Using either sensor method (in vitro or in vivo), the assay time of the present invention is dependent upon the concentration of protease present in the sample or tissue. The cleavage speeds will increase by 3-5 times per order of magnitude of increase in protease concentration. In the presence of an aggressive tumor, assay time can be as fast as a fraction of a second. In healthy tissue, it can take about 24 hours for activity to be detected. Thus, the faster the assay, the more aggressive the tumor, and the greater the likelihood of metastatic potential of the tumor. The use of protease-specific oligopeptides for the construction of a nanoparticle-based in vivo nanosensors for the determination of the metastatic potential of solid tumors has never been done before. Preferably, when the assay is directly injected into the tumor region (or suspected tumor region), results can be determined about 30 minutes after injection. When the assay is administered intravenously, the results can be read within about 1 hour after administration of the IV (to permit the assay to reach the target region), and up to 24 hours after administration. In either case, once the assay is in the vicinity of the tumor, protease activity detected within 10 minutes can be correlated with a high probability that the tumor is aggressive. Preferably, if no activity is detected within the first 30 minutes, there is a very low probability that the tumor is aggressive. Likewise, for in vitro testing protease activity detected within 10 minutes can be correlated with a high probability that the tumor is aggressive, whereas no activity within the first 30 minutes after contacting the sample with the assay can be correlated with a very low probability that the tumor is aggressive. This reaction rate provides a distinct advantage over known detection methods which take several hours for assay completion (and results).

EXAMPLES

The following examples set forth preferred methods in accordance with the invention. It is to be understood, however, that these examples are provided by way of illustration and nothing therein should be taken as a limitation upon the overall scope of the invention.

EXAMPLE 1

Synthesis of Nanoparticle Assembly

In this procedure, the synthesis of a nanoparticle assembly is described. The nanoparticles can be synthesized according to known methods. They are also commercially-available from various sources, for example from Nanoscale Corp. (Manhattan, KS) and Sigma Aldrich (St. Louis, MO). Suitable nanoparticles for use in the following method include freshly-prepared, non-stabilized nanoparticles, or stabilized nanoparticles. Non-stabilized nanoparticles can be stabilized using ligand exchange as described below.

1. Ligand Exchange

A first set of nanoparticles are dissolved in a non-polar or dipolar aprotic solvent and then treated with 2-aminoethanethiol under pressure (1000 psi) at room temperature for 1 hour. Alternatively, water-soluble nanoparticles can be treated with 2-aminoethanethiol in H_2O/acetonitrile mixtures under pressure (1000 psi) at room temperature for 1 hour.

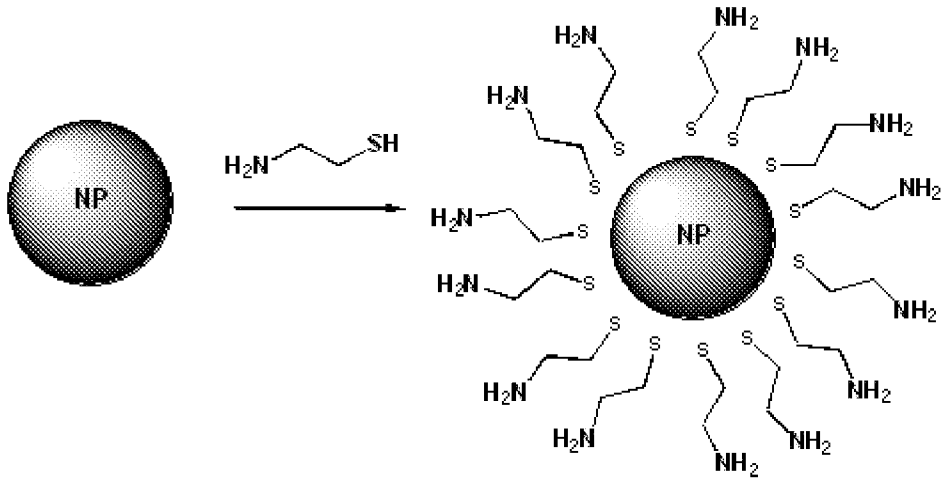

The surface-exchanged nanoparticles are then isolated using preparative Gel Permeation Chromatography (HPLC).

2. Preparation and attachment of oligopeptide to second nanoparticle

The consensus sequence (cleavage sequence) of the target protease is then selected, and the oligopeptides containing the consensus sequence for coupling the nanoparticles is prepared by using classic peptide synthesis (modified Merrifield synthesis). These oligopeptides are also commercially available from numerous companies such Genscript (Piscataway, NJ). The sequence ends with a cysteine on the C-terminal end for reacting with a second set of (non-exchanged) nanoparticles via the thiol group. Its N-terminus is used to react with the first set of surface-exchanged nanoparticles described above. To enhance the binding of the N-terminal end to the second nanoparticle, up to 2 lysine residues can also be added to this end of the oligopeptide. An exemplary oligopeptide structure is illustrated below with one lysine residue attached to the N-terminus of the peptide sequence.

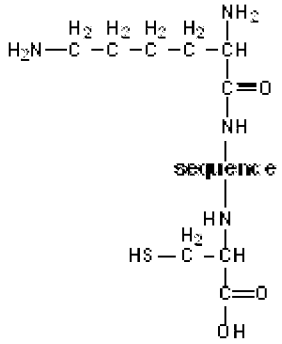

A second set of non-exchanged nanoparticles are then reacted with the oligopeptides in a non-polar, or dipolar aprotic solvent, or aqueous buffer at room temperature under N_2 or argon atmosphere for 24 hours. The addition of $NaBH_4$ to the reaction solution ensures that the cysteine units of the oligopeptide do not form disulfide bonds. This reaction has to be performed under dilution conditions (concentration < 10^{-5}M) to enable the formation of 1:1 adducts (nanoparticle-oligopeptide) with high yields.

3. Coupling of the first and second nanoparticles

To link the two nanoparticles, the surface-exchanged nanoparticle is first treated with carbonyl-bis-imidazol (CDI) in dimethylformamide (DMF) at 40°C for 1 hour in highly concentrated solution.

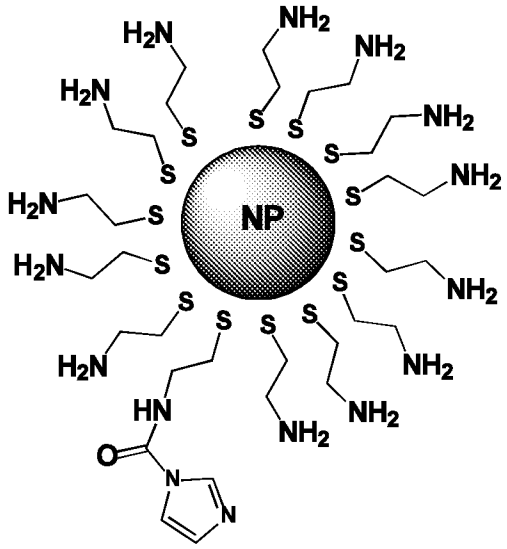

CDI-treated surface-exchanged nanoparticle

The treated surface-exchanged nanoparticle is then be added to the non-exchanged nanoparticle-oligopeptide mixture described above. The probability of binding the N-terminal end of the oligopeptide to the surface-exchanged nanoparticle can be enhanced by attaching up to two lysine-residues to the N-terminal end of the oligopeptide linkage.

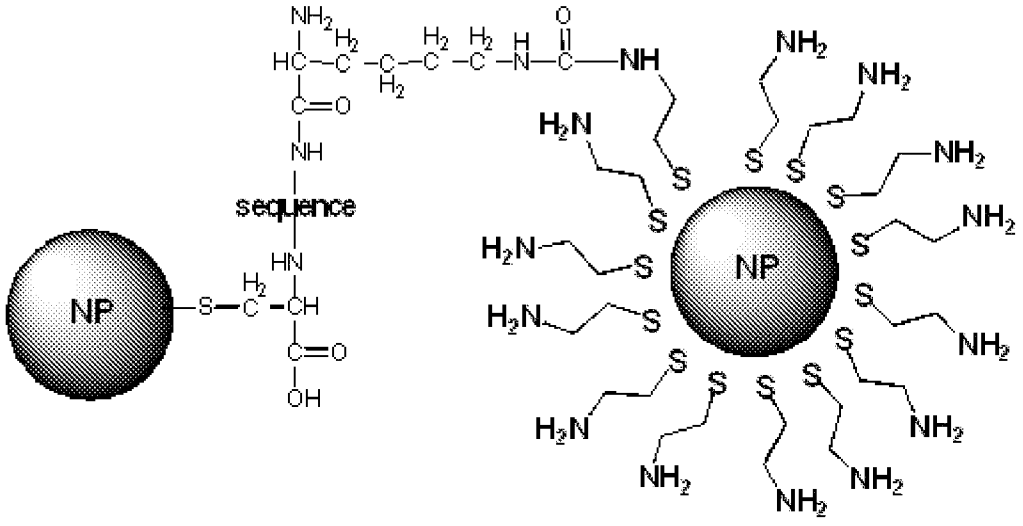

4. Surface-exchange treatment of non-exchanged nanoparticle

Finally, the second nanoparticle is treated with 2-aminoethanethiol under high pressure (1000 psi) at room temperature for 1 hour. Alternatively, water-soluble nanoparticles can be treated with 2-aminoethanethiol in H_2O/acetonitrile mixtures under pressure (1000 psi) at room temperature for 1 hour.

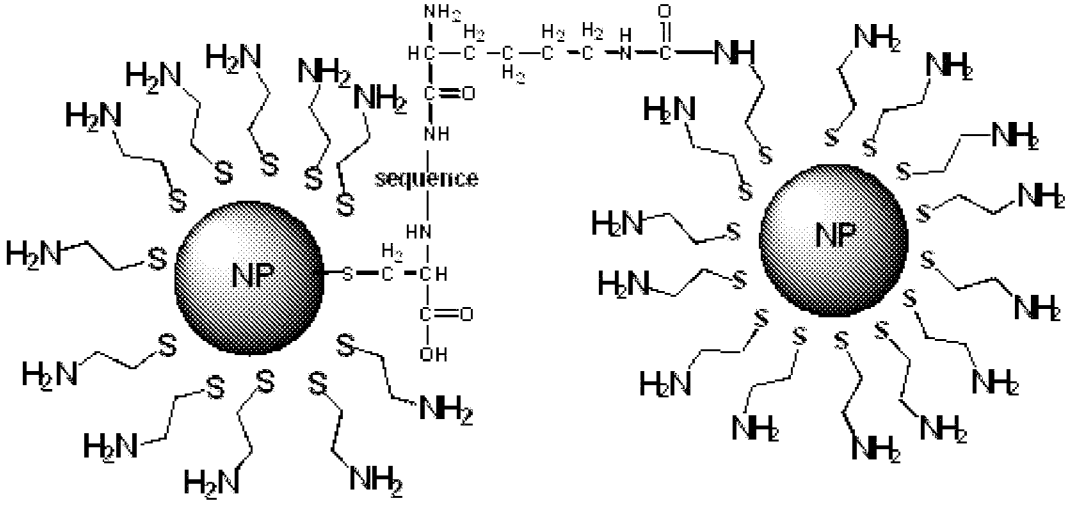

A fraction of the amino groups bind a proton and are negatively charged at pH=7 in aqueous environments. This ensures that the nanoparticles repel each other and the maximal distance is kept, to avoid clustering of the nanoparticles during the assay.

The foregoing procedure can be followed to synthesize nanoparticle assemblies using metal nanoparticles (e.g., Au, Ag, Pt, etc.), nanoparticle-alloys (e.g., AuCu, FePt, CoFe, AuFe, etc.), and core/shell nanoparticles.

EXAMPLE 2

Preparation of Dye Assemblies

In this procedure, the synthesis of dye assemblies is described. The consensus sequence (cleavage sequence) of the target protease is selected. The oligopeptide containing the consensus sequence for coupling the dyes is then prepared by using classic peptide synthesis (modified Merrifield synthesis), resulting in an exemplary oligopeptide as shown in Example 1. Virtually any fluorescent or phosphorescent dye is suitable for

linking to the oligopeptide. However fluorescent dyes or phosphorescent metal complexes possessing a high fluorescence or phosphorescence quantum yield are more suitable. There must be an overlap between the excitation spectrum of the first dye and the fluorescence or phosphorescence spectrum of the second dye in the assembly to permit Förster Energy Transfer (see below). Examples of suitable dyes include all coumarins (especially suited to one- and multi-photon excitation), porphyrins and related compounds, fluoresceine and related compounds, ruthenium polypyridyl complexes, as well as other fluorophores and metal complexes described herein.

The fluorophore or phosphorescent metal complex is linked via an amino-group to a spacer featuring one carboxyl group and one thiol group. The carboxyl group is then used to make a stable amide-bond with the dye. The thiol group is used to link the dye to the C-terminal cysteine group of the oligopeptide. First, the dye is reacted with the spacer using dicyclohexyl-carbodiimide (DCC) with N-hydroxysuccinimide (NHS) as shown below.

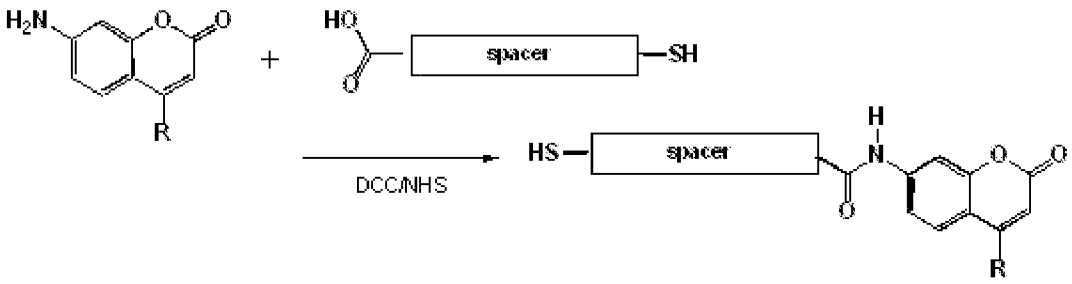

The spacer-attached dye is then reacted with the oligopeptide in a non-polar, or dipolar aprotic solvent or aqueous buffer at room temperature under N_2 or argon atmosphere for 24 hours. The addition of $NaBH_4$ to the reaction solution ensures that the cysteine units do not form disulfide bonds. This reaction has to be performed under dilution conditions (concentration < 10^{-5}M) to enable the formation of 1:1 adducts (dye-oligopeptide) with high yields.

Alternatively, the dye can be linked to the N-terminal end of the oligopeptide. In this case, the spacer features two carboxyl groups as shown below.

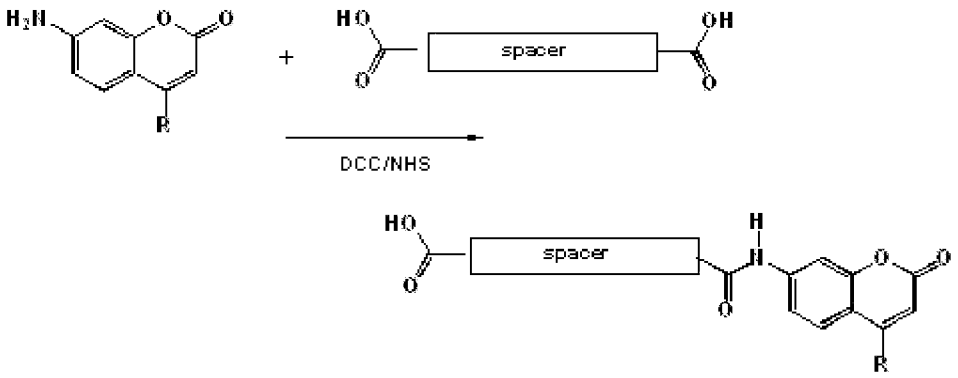

The separation of the final product is performed using reverse-phase (C18) chromatography.

Other fluorophores and metal complexes are linked according to the same methodology, as shown in the examples below.

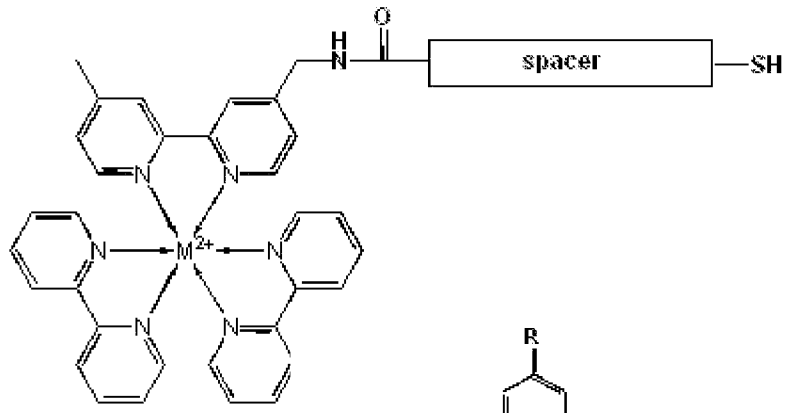

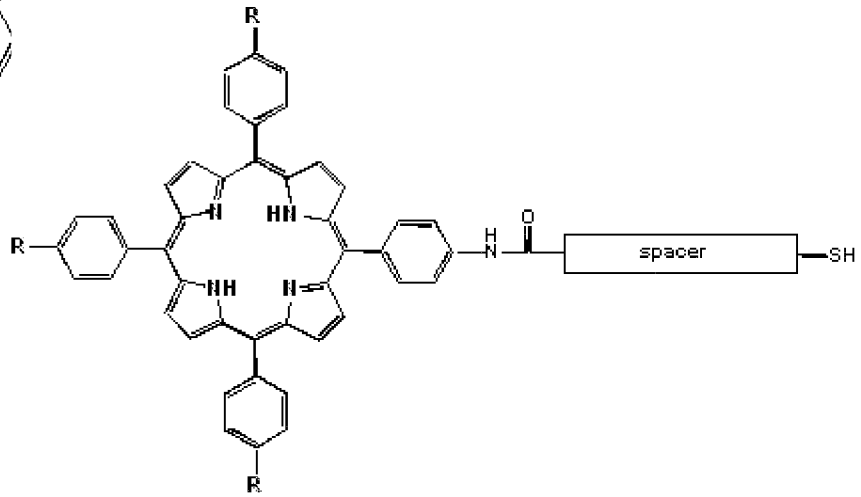

where R = -COOH or $N(R^1)_3$, where each R^1 is selected from the group consisting of -H, alkyls, and aryls.

EXAMPLE 3

Nanoparticle-Nanoparticle: Absorption Spectroscopy

In this procedure, UV/Vis-Absorption spectroscopy was used to measure the activity of uPA. All chemicals and solvents were purchased from Fisher/Acros (Pittsburgh, PA), unless otherwise noted. A nanoparticle-nanoparticle assembly was prepared using citrate-stabilized gold nanoparticles (Sigma-Aldrich, St. Louis, MO) with a 10 nm diameter and an oligopeptide with the following sequence: CGGG**SGRSA**GGGC (SEQ ID NO: 35) (GenScript, Piscataway, NJ). First, 1 mg of the nanoparticles was suspended in 25 ml of tetrahydrofuran (THF) containing 1.0 x 10^{-3} M of glycine. The microheterogeneous solution was heated under pressure (100 psi) and argon-atmosphere to 200 °C for 5 hours. The reaction was carried out using a High-Pressure Reactor (available from Parr Instruments, Moline, IL). Digestive ripening decreased the Au-nanoparticle diameter to 4-5 nm. The nanoparticles were then removed from the solution by ultracentrifugation at 30,000 rpm and then resuspended in THF. The procedure was repeated 10 times to remove all non-bonded glycine.

Next, 0.1 mg of the oligopeptide was added to the Au-nanoparticles in 1.0 ml of anhydrous THF, followed by stirring for 24 hours. The oligopeptide and nanoparticles were precipitated by centrifugation at 30,000 rpm and then resuspended in THF. This procedure was repeated 10 times. The linked Au-Au nanoparticle assemblies were then dissolved in phosphate buffer (PBS; pH=7.02), precipitated by centrifugation at 20,000 rpm and resuspended again in PBS.

The reported absorption coefficient at the maximum absorption of the plasmon is $\varepsilon = 7.66 \times 10^{9}\ M^{-1}cm^{-1}$. This absorption coefficient was used to estimate the concentration of the Au-Au nanoparticles at $1x10^{-4}$ mol.

The Au-Au nanoparticles in PBS solution were then added to a quartz cuvette (~3.0 mL). The solution was heated to 37°C for 15 minutes. Next, $1x10^{-8}$ mol of urokinase in 0.050 ml of PBS (Innovative Research, Inc., Novi, MI) was added to the cuvette.

The spectral shift in the plasmon absorption of the coupled pair of gold nanoparticles before, during, and after urokinase cleavage of the oligopeptide is shown in Figure 2. An Agilent 8453 UV-Visible spectrophotometer, equipped with a temperature

bath was used to measure the changes in the emission spectrum. The maximum of the gold plasmon absorption was observed to shift from 523 nm to 517 nm within 180 seconds. It is also apparent that the intensity of the plasmon absorption greatly varies at 515 nm (increase) and 525 nm (decrease). The quotient of both measurements will be able to provide reliable time-resolved measurements of the urokinase activity. Urokinase can serve as a model for all proteases shown in Table I.

EXAMPLE 4

Fluorescence/Phosphorescence Assays

Chromophore-Chromophore Assemblies

In this example, fluorescence/phosphorescence assays were used to measure activity of uPA. A chromophore-chromophore assembly was prepared using the peptide sequence SRSRSRSRSR**SGRSA**GGGC (SEQ ID NO: 18) (GenScript) as a spacer between a pyrene fluorophore and a coumarin acceptor. All chemicals and solvents were purchased from Fisher/Acros (Pittsburgh, PA), unless otherwise noted. The assembly was prepared by dissolving 0.00010 mol of coumarin in THF at room temperature. Next, 0.00012 mol of 1-ethyl-3-(3-dimethyllaminopropyl) carbodiimide (EDC) were added as solid under argon-atmosphere and allowed to react for 5 hours. Then, the oligopeptide linkage was attached to the coumarin by adding to the reaction 0.00010 mol of the oligopeptide dissolved in 1 ml bidest. (double purified) water, followed by stirring at room temperature for 24 hours under argon atmosphere. Next, 0.0020 mol of mercaptopyrene was added as a solid to the solution, and completely dissolved within 5 minutes. The solution was continuously stirred under ambient conditions for another 24 hours.

The solvent was then removed in vacuum and the assembly was purified by HPLC using a reverse phase (C18) column chromatography with acetonitrile and PBS as eluent. The resulting chromophore-chromophore assembly is shown below.

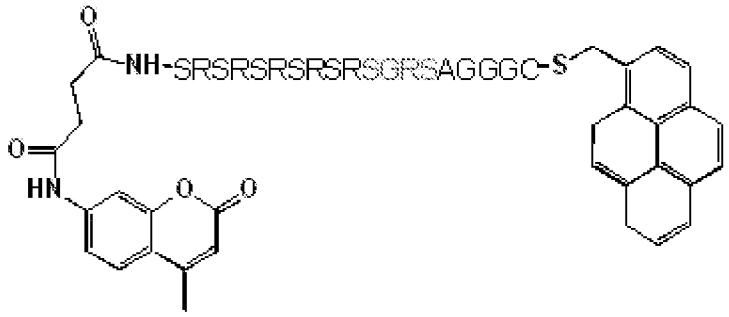

Coumarin Pyrene

The nanoplatform assembly (1 x 10^{-6} mol) in PBS was added to a quartz cuvette (~3 mL). The solution was heated to 37°C for 15 minutes. Then about 1 x 10^{-8} mol urokinase in 0.050 ml PBS (Innovative Research) was added to the cuvette.

The spectral shift from the assay is depicted in Figure 3. The changes in the emission spectra were measured using a spectrofluorometer (ISA-SPEX, Fluoromax-2; ISA, Inc., Edison, NJ). Upon photoexcitation of the pyrene at 280 nm, FRET occurs, which causes the attached coumarin to emit most of the phosphorescence/luminescence. The urokinase cleaves the oligopeptide linker between the two chromophores, which drastically changes the observed spectrum. The spectra shows assay time over 0, 2, 4, 6, 8, 10, and 15 minutes. The coumarin emission decreases with time because FRET decreases when the oligopeptide linker is cleaved by urokinase, and the distance between the coumarin and pyrene molecules increases.

EXAMPLE 5

Stealth-Protection and Optimization of the Porphyrin-Content and -Composition

In this example, stealth ligands featuring chemically-attached metalated and unmetalated tetracarboxy-phenyl-porphyrin (TCPP) were linked to core/shell Fe/Fe_3O_4-nanoparticles (NanoScale Corporation; Manhattan, KS) with oligopeptide linkers. Using porphyrins, two different urokinase-sensors can be created.

1. FRET-Based Sensor

For the FRET-Based Sensor, five Zn-TCPP porphyrins were attached to one central stealth-protected Fe/Fe_3O_4 nanoparticle, and then a non-metalated TCPP porphyrin was attached to the central nanoparticle, using the procedure described below.

To prepare the stealth-protected Fe/Fe_3O_4-nanoparticles, 35 mg of dopamine-tetraethylene glycol ligand were dissolved in 5 ml THF. Next, 11.0 mg of Fe/Fe_3O_4-nanoparticles were added and sonicated at room temperature for 1 hour. The core of the nanoparticles had a diameter of from about 3-5 nm. The Fe_3O_4 shell had a thickness of less than 2 nm. The solid was then collected with a magnet and solvent was decanted carefully. The solid was washed with THF (3×3 ml). After drying under vacuum for 2 hours, 10.0 mg of stealth-protected nanoparticle product was obtained.

The oligopeptide linker was then attached to the metalated porphyrin. First, 5.0 mg of the porphyrin was refluxed in 5.0 ml $SOCl_2$ at 100 °C for 30 minutes. The excess $SOCl_2$ was then removed under high vacuum, and the resulting solid was further dried under vacuum for 3 hours. Next, 4 mg of the oligopeptide sequence CGGGSGRSAGGGC (SEQ ID NO: 35) and 5 ml THF were added to the porphyrin solid and stirred at room temperature for 5 hours. The THF was then removed under vacuum, and a greenish-colored solid was obtained. Electrospray ionization (ESI) mass spectrometry showed a mixture of at least 2 linked porphyrin species (mono-peptide and di-peptide linked to porphyrin). The procedure was repeated to attach the oligopeptide linker to the non-metalated porphyrin.

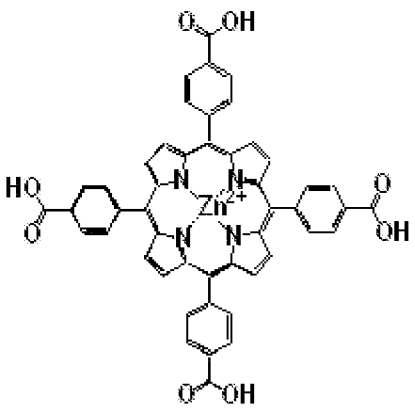

Zn-TCPP (P_1)

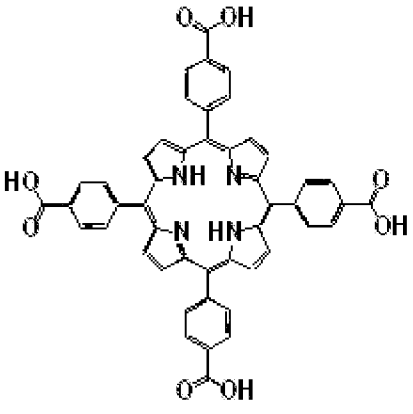

Non-metalated TCPP (P_2)

To attach the porphyrins to the nanoparticles, the metalated porphyrin-oligopeptide solid was dissolved in 10 ml dry THF. Next, 5.0 ml of this solution was added to 10.0 mg of the dopamine tetraethylene glycol-tethered Fe/Fe_3O_4 nanoparticles, followed by 1.0 mg 4-dimethylaminopyridine (DMAP) and 8.0 mg EDC. The resulting suspension was sonicated for 1 hour at room temperature. The solid precipitate was collected by magnet and thoroughly washed with THF (8×2 ml). The sample was then dried under high vacuum for 5 hours. 8.0 mg of product was obtained. The procedure was repeated to attach the non-metalated porphyrin to the nanoparticle.

The emission spectra of the nanoplatform assembly ($1x10^{-5}$ M) in PBS in the presence of about $1x10^{-8}$ M urokinase is depicted in Figure 4, at 0 (A), 2 (B), 4 (C), and 6 minutes (D). The release of the oligopeptide-tethered TCPP from the Fe/Fe_3O_4-nanoparticle by urokinase is visible from the distinct decrease of the fluorescence band at λ_1= 607 nm. The concentration dependence of the fluorescence occurring from the other two fluorescence bands (at λ_2= 654 nm, λ_3= 718 nm) was observed to be non-linear. The reason for the observed non-linear behavior can be found in the high fluorescence quantum yield of the untethered, non-metalated TCPP. We estimated Φ=0.082, which is approximately eight times higher than in the tethered state, when the large porphyrin-concentration in the sphere around the Fe/Fe_3O_4-nanoparticle leads to increase FRET and, consequently, radiation-less deactivation of the excited states.

In Figure 5, the ratios of the integrals of the fluorescence bands shown at λ_1= 607 nm, λ_2= 654 nm, and λ_3= 718 nm are plotted versus the mol percent of released TCPP (as measured by HPLC using an Agilent workstation (HP 1050) equipped with an optical detection system). The plots of $R=I(l_2)/I(l_1)$ and $R=I(l_3)/I(l_1)$ increase with increasing mol percent of released TCPP. The plots are quite linear in the concentration range from 0 to 7 mol percent released TCPP. Therefore, the concentration of TCPP that is released by urokinase, can be measured by recording fluorescence spectra of the nanoplatform at different time intervals and comparing the fluorescence intensities at the three wavelengths (λ_1, λ_2, λ_3). It should be noted that all three wavelengths permit in vivo-measurements in mammalian tissue, especially when coupled with single-photon counting techniques (e.g., fluorescence microscopy).

In this example, tetracarboxy-phenyl-porphyrin (TCPP) was used, but virtually any organic chromophore, metalated chromophore, or quantum dot (e.g., ZnS-stabilized CdSe) can be employed and attached to the nanoparticle via the oligopeptide linker.

Another oligopeptide sequence that was tested using this assembly is KGGSGRSAGGD (SEQ ID NO: 41).

2. "Light-Switch" for Detecting Protease Activity

This type of urokinase sensor is based on the quenching of the excited states of chromophores (e.g. porphyrins) with organic (e.g. viologens) or inorganic quenchers (e.g. metal, alloy, and core/shell nanoparticles). Due to the proximity of the nanoparticles (~ 2 nm) to the chromophore, the surface plasmon of the core/shell nanoparticle is able to quench the emission spectra from the chemically-attached porphyrin. Once released by urokinase cleavage, the fluorescence or phosphorescence of the chromophore increases significantly. This fluorescence increase can be detected spectrally. When several chromophores featuring discernible emission spectra are used, the activity of various enzymes can be detected simultaneously. The assembly is prepared using the same procedures described above for the FRET-based sensor, except that only one type of porphyrin was used (i.e., non-metalated only or metalated only). This mechanism is depicted below using a bimagentic-nanoparticle linked to a dopamine-tetraethylene glycol ligand featuring a chemically-linked non-metalated TCCP porphyrin with the oligopeptide sequence DGGSGRSAGGK (SEQ ID NO: 36).

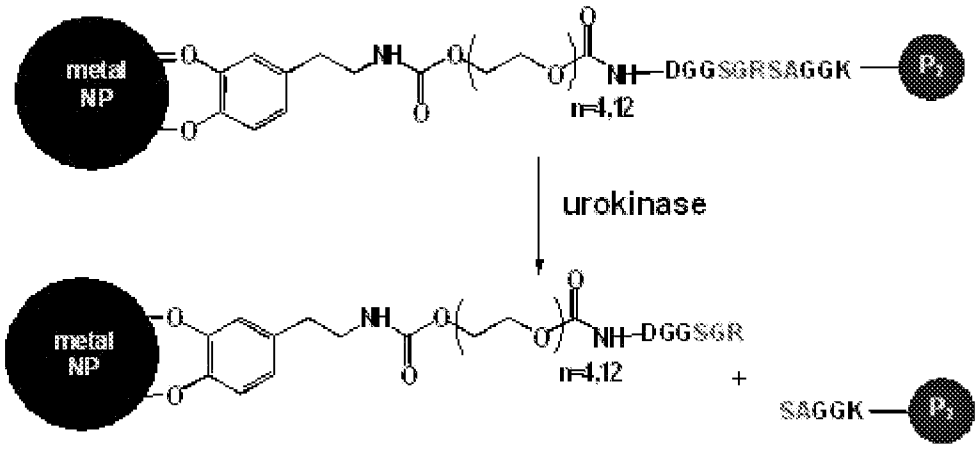

The light-switch mechanism was tested using 3 samples of urine from rats impregnated with MATB III type cancer cells (rodent model for aggressive breast cancer), since urokinase can pass the mammalian kidneys and retains at least some activity in urine. The samples were collected 36, 15, and 5 days after cancer impregnation, respectively, and immediately frozen at -80°C. The tests on the day 36 sample were run twice. Before testing, the urine samples were thawed and allowed to come to room temperature. The following procedure was used to test each sample.

The TCPP-nanoparticle nanoplatform assembly was dissolved in bidest. water using sonication for 30 minutes. Next, 100 µl of urine was added 2.0 ml of the water solution containing 0.1 mg of the nanoplatform. The temperature was kept constant at 34°C. The fluorescence spectra was recorded every 2 minutes for the 36 day and 5 day samples, and ever 1 minute for the 15 day sample.

As can be seen from Figure 6, the luminescence from TCPP increased steadily over time for the 36 day urine. Figure 7 shows the plot of the relative intensities of the luminescence of TCPP occurring at λ=656 nm using the measurement shown in Figure 6.

Figure 8 shows the plot of the relative intensities of the luminescence of TCPP occurring at λ=656 nm from the 15 day sample.

The rat urine which was collected only 5 days after impregnation of the rats with MATB III tumor cells, does not show any discernible urokinase activity, as shown in

Figure 9. The urine data correlates nicely with the observed growth curves of MATB III tumors in rats, where the maximum of tumor growth can be discerned approximately 2 weeks after the impregnation of the MATB III cells. However, after stem cell therapy, the tumors are significantly attenuated by day 36.

EXAMPLE 6

Quantum dot assemblies

In this example, the preparation of nanoplatform assemblies of CdSe/ZnS core/shell quantum dots linked to gold coated Fe_2O_3 nanoparticles is described. The CdSe/ZnS quantum dots will be in their 'OFF' state when initially attached to the gold surface of the nanoparticle, due to the quenching effects of the nanoparticle. Once the oligopeptide is cleaved by the enzyme urokinase, the CdSe/ZnS is released and becomes fluorescent. This enzyme-triggered light switch indicates the presence of the target enzyme. An Au/Fe alloy nanoparticle can also be used instead of the Fe_2O_3 nanoparticles.

1. Synthesis of Quantum Dots

Synthesis of CdSe/ZnS quantum dots is well established. The synthesis takes place at 120°C in hexadecyl amine using a single precursor $Li_4[Cd_{10}Se_4(SPh)_{16}]$ to form the CdSe core. The precursor slowly decomposes over many hours resulting in high quality crystals. Once the synthesis is complete, the ZnS shell is grown over the CdSe core as indicated by an in situ photoluminescence technique at high temperature, allowing very sensitive control over the reaction conditions. The growth of the quantum dots is shown by the shift of the photoluminescence (PL) emission maximum, as depicted in Figure 10. When the quantum dots are heated to 250°C, the emission of the uncoated quantum dots is strongly quenched. At the overcoating step, the emission of the quantum dots reappears, even at 250°C.

Quantum dots have very large photoluminescence yields along with very large absorption cross-sections, which decreases the thermal load on the biological system. If different color emission is needed for creating multiple sensors (multiplex detection) this can be achieved by changing the size of the quantum dot core yielding different emission wavelengths. CdSe can be easily tuned between 500-650 nm with size change. While

these quantum dots can be grown to virtually any size, the growth of the quantum dots will be restricted to less than 5.5 nm so that the nanoplatform can efficiently leave the filtration system of the body (renal pathway) when used in vivo.

2. *Stabilization of Quantum Dots*

Although CdSe/ZnS quantum dots are sufficiently stable towards bio-corrosion, the binding of an amphiphilic resorcinarene-ligand will greatly enhance their water-solubility and enable the binding of the oligopeptide sequence containing the protease consensus sequence, especially when the following sequences are utilized: a) KGGGSGRSAGGGC for urokinase; b) KGGVPMS-MRGGGC, for MMP1; c) KGGIPVS-LRSGGC for MMP2; and d) KGGVPLS-LTMGGC for MMP7, where "-" indicates the point of protease cleavage. The ligand creates a monolayer shell around the quantum dot. A preferred resorcinarene ligand for quantum dot stabilization (as well as nanoparticle stabilization) is illustrated below.

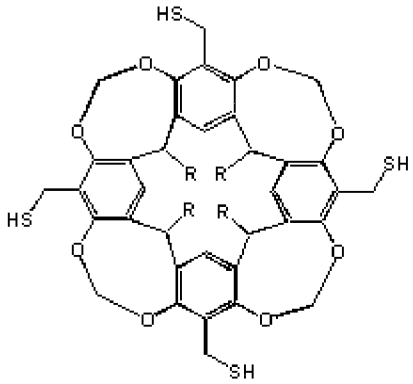

macrocyclic calixarene ligand

where: R = 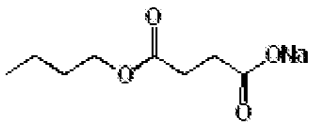

The monolayer can be formed on the quantum dot surface in either a non-aqueous liquid (e.g., THF, DMF, acetonitrile) or in an aqueous buffer (e.g., PBS, water/THF-mixtures, or water-alcohol-mixtures), depending on the selected synthesis route of the quantum dot (or nanoparticle). A nanoparticle or quantum dot of 5 nm in diameter requires 55 resorcinarene ligands for the formation of a monolayer. The ligand is amphiphilic (logP=4.7).

3. Attachment of Oligopeptides to Stabilized Quantum Dot

The next step in the assembly of the nanoplatform will be the chemical attachment of the oligopeptide linkers to the pendant carboxylic acid groups at the "feet" of the resorcinarene-ligands, which are stabilizing the CdSe/ZnS quantum dots. The oligopeptides are commercially available. Binding of the terminal lysine residue of the oligopeptide to the resorcinarene-carboxylates will be achieved by using the well-known DCC/NHS/HOBT-method, which is a standard procedure in protein synthesis and bioconjugation. Each cleavage sequence will be bound to one particular quantum dot featuring a distinct luminescence maximum (blue, green, yellow, or red depending upon size), allowing for multiplex detection of enzyme activity. The separation of the quantum dots from the reaction solvent will be achieved by centrifugation. After linking, the quantum dot is then transferred stepwise into an aqueous buffer (PBS) again.

Electrospray/time-of-flight mass spectrometry is suitable for determining the total mass of the assemblies, which permits the determination of the surface coverage of the oligopeptides over the surface of the stabilized quantum dot. It is important that the layer of attached oligopeptides featuring the cleavage site is somewhat incomplete (max. of about 75 percent surface coverage) to permit the attack of target protease (e.g., urokinase), which would be impeded by sterical factors if a perfect coverage is achieved (although the DCC/NHS/HOBT method may not be efficient enough to permit such coverage). An extra HPLC-step will be used to obtain highly pure oligopeptide. The oligopeptide coverage over the surface of the quantum dot can be varied systematically, beginning with 25% surface coverage. The EDC/NHSS-method, which is adapted for protein synthesis and bioconjugation in aqueous solvents can also be employed.

4. Attachment of the Quantum Dots to the Gold Coated Iron Oxide Nanoparticle

Next, the CdSe/ZnS quantum dots are linked to the Fe_2O_3/Au nanoparticles via the cysteine residue on the C-terminal end of the oligopeptide linkers. To determine the activity of one enzyme, one kind (size) of quantum dot will be linked to the nanoparticle. However, for the *in vivo* determination of cancer progression, up to four different quantum dots (featuring different oligopeptide sequences) will be bound to a single gold coated nanoparticle. This reaction is carried out by binding the terminal cycseine-residues of the

cleavage sequence to the gold shell around the iron oxide nanoparticle. Molecular modeling was used to determine that the length of each of the four oligopeptides will be less than 4.5 nm. Therefore, the total distance between the Fe_2O_3/Au nanoparticle and stabilized CdSe/ZnS quantum dot will be approximately 5 nm (i.e., resorcinarene ligand + oligopeptide linker), which is the optimal distance for maximal luminescence quenching of the quantum dots by the Au nanoshell when tethered.

EXAMPLE 7

Test of an In-Vivo Sensor for Urokinase Using Fluorescence Microscopy

The in-vivo urokinase-assay was tested in Charles River female mice, which have been impregnated with B16F19 mouse melanoma cells 10 days prior to these measurements. The mice were anesthetized and then a solution of a Fe/Fe_3O_4-nanoparticle-TCPP assembly was administered to the mice intravenously (IV) or via direct injection into the tumors (IT). The IV solution was 200 μg of the nanoparticle assembly in 200 ml PBS. The IT solution was 100 μg of the nanoparticle assembly in 200 ml PBS. To measure the activity of the assay, the mice were anesthetized again and placed under a fluorescence microscope employing a single-photo-counting detector. This instrument has been built in-house. The results of the single-photo-counting spectra, from the right and left limbs of the mice, recorded through a fluorescence microscope (resolution: 1 m x 1 m x 1 m) is illustrated in Figure 11 (red: left limb; blue: right limb). Box A shows the results from mouse 1, which was IT-injected 30 minutes prior to measurement. Box B shows the results from mouse 2 (no tumors), which was IV-injected 12 hours prior to measurement. Box C shows the results from mouse 3 (bearing tumors on both legs), which was IV-injected 12 hours prior to measurement. Box D shows the results of mouse 4, which was IV-injected 24 hours prior to measurement. Box E shows the results from the control mouse, neither IT- nor IV-injected. Box F is a repeat of C from mouse 7.

The tumor regions at the hind legs of the mice were excited using laser light (Ti:sapphire-laser, λ =870 nm, P=6.5 mW) in the IR-region. TCPP requires tri-photonic excitation at this excitation wavelength. It is remarkable that the signal strengths obtained in the right legs of the tumor-bearing mice correlates with the tumor size, whereas the

signal in the left limb apparently does not. The hypothesized explanation is that the uptake of the nanoparticle assembly by the tumors is so quick, that the first tumor, which is encountered by the injected intravenously, incorporates almost everything. It was found that the IT-injection is less efficient than IV-injection, because the urokinase does not have the time to cleave the majority of the cleavage sequences and the porphyrin does not light up.

EXAMPLE 8

Measurements of Urokinase Activity in PBS

In this example, a calibration curve was recorded to demonstrate how urokinase activity (as a model for all proteases discussed herein) changes with increasing urokinase concentration. The changes in the emission spectra were measured using a spectrofluorometer (ISA-SPEX, Fluoromax-2; ISA, Inc., Edison, NJ). All chemicals and solvents were purchased from Fisher/Acros, unless otherwise noted.

The pH of the urine of a healthy rat is 6.7±0.4. Therefore, the curve was recorded in PBS (pH= 6.8) using four concentrations of urokinase: $1x10^{-10}$ M, $1x10^{-9}$ M, $5x10^{-8}$ M (2x) and $1x10^{-8}$ M. Fe/Fe_3O_4 nanoparticle-TCPP assemblies featuring the urokinase cleavage sequence were dissolved in PBS. The nanoparticle assembles were first dissolved in water at a concentration of 0.5mg of nanoparticles per 1ml of water, followed by sonication for 30 minutes to render the nanoparticles soluble in the water. Next, 2.0ml of water containing 0.1 mg of the nanoplatform was mixed with the PBS. The temperature was kept constant at 34°C. Continuous excitation was done at 417 nm. Fluorescence spectra were recorded at constant time intervals (10min, 5min, 2min or 1min, depending on the concentration. The urokinase was then added to the PBS mixture. The emission band at 656 nm was monitored.

The results are shown in Figure 12, where k is the rate constant obtained by plotting (I: luminescence intensity)/(I_0: luminescence intensity prior to adding urokinase) vs. time (in seconds). As can be seen from the graph, the cleavage rate increases by 3-5 times per order of magnitude of increase in urokinase concentration. Thus, the speed of cleavage can be correlated with the aggressiveness of the tumor.

We Claim:

1. A nanoplatform assembly for detecting protease activity comprising:

a first particle;

a second particle; and

a linkage between said first and second particles, wherein said linkage comprises a protease consensus sequence.

2. The assembly of claim 1, wherein said first and second particles each have respective diameters of from about 1 to about 100 nm.

3. The assembly of any one of claims 1-2, wherein said first and second particles are each individually selected from the group consisting of nanoparticles, chromophores/luminophores, quantum dots, viologens, and combinations thereof.

4. The assembly of any one of claims 1-3, wherein said first and second particles are non-identical.

5. The assembly of any one of claims 1-4, wherein said first and second particles are both nanoparticles, chromophores/luminophores, or quantum dots.

6. The assembly of any one of claims 1-5, wherein at least one of said particles is a nanoparticle.

7. The assembly of claim 6, wherein said nanoparticle comprises a metal selected from the group consisting of elemental metals and metal salts, said metal salts being selected from the group consisting of oxides, sulfides, selenides, and tellurides.

8. The assembly of claim 6, wherein said nanoparticle comprises an alloy of two or more metals.

9. The assembly of claim 6, wherein said nanoparticle comprises a metal selected from the group consisting of gold (Au), silver (Ag), copper (Cu), nickel (Ni), palladium (Pd), platinum (Pt), cobalt (Co), rhodium (Rh), iridium (Ir), iron (Fe), ruthenium (Ru), osmium (Os), manganese (Mn), rhenium (Re), scandium (Sc), titanium (Ti), vanadium (V), chromium (Cr), zinc (Zn), yttrium (Y), zirconium (Zr), niobium (Nb), molybdenum (Mo), technetium (Tc), cadmium (Cd), lanthanum (La), lutetium (Lu), hafnium (Hf), tantalum (Ta), tungsten (W), actinium (Ac), lawrencium (Lr), rutherfordium (Rf), dubnium (Db), seaborgium (Sg), bohrium (Bh), Hassium (Hs), meitnerium (Mt), darmstadtium (Ds), roentgenium (Rg), ununbium (Uub), selenium (Se), and the oxides, hydroxides, sulfides, selenides, and tellurides of the foregoing, and combinations thereof.

10. The assembly of claim 9, wherein said oxides are selected from the group consisting of FeO, Fe_3O_4, Fe_2O_3, Fe_xO_y, CuO, NiO, Ag_2O, and Mn_2O_3.

11. The assembly of claim 6, wherein said nanoparticle is a core/shell nanoparticle comprising a metal or metal-alloy core and a metal shell.

12. The assembly of claim 11, wherein said core is selected from the group consisting of Au, Ag, Cu, Co, Fe, and Pt.

13. The assembly of any one of claims 11-12, wherein said shell is selected from the group consisting of Au, Ag, Cu, Co, Fe, Pt, the metal oxides thereof, and combinations thereof.

14. The assembly of claim 11, wherein said core/shell nanoparticle is selected from the group consisting of Fe/Au, Fe/Fe_3O_4, and Au/Fe_2O_3.

15. The assembly of any one of claims 11-14, wherein said core has a diameter of from about 1 nm to about 25 nm.

16. The assembly of any one of claims 11-15, wherein said shell has a thickness of from about 0.5 nm to about 10 nm.

17. The assembly of any one of claims 6-16, wherein said nanoparticle is a stabilized nanoparticle comprising an organic monolayer surrounding the nanoparticle.

18. The assembly of claim 17, wherein said monolayer is comprised of ligands.

19. The assembly of claim 18, wherein said ligands comprise at least one member selected from the group consisting of thiols, alcohols, nitro compounds, phosphines, phosphine oxides, resorcinarenes, selenides, phosphinic acids, phosphonicacids, sulfonic acids, sulfonates, carboxylic acids, disulfides, peroxides, amines, nitriles, isonitriles, thionitiles, oxynitriles, oxysilanes, alkanes, alkenes, alkynes, aromatic compounds, and seleno moieties.

20. The assembly of any one of claims 17-19, wherein said monolayer is selected from the group consisting of alkanethiolate monolayers, aminoalkylthiolate monolayers, alkylthiolsulfate monolayers, and organic phenols.

21. The assembly of any one of claims 17-20, wherein said nanoparticle is selected from the group consisting of trioctyl-phosphinoxide-stablized nanoparticles, amine-stabilized nanoparticles, carboxylic-acid-stabilized nanoparticles, phosphine-stabilized nanoparticles, thiol-stabilized nanoparticles, aminoalkylthiol-stabilized nanoparticles, and organic phenol-stabilized nanoparticles.

22. The assembly of any one of claims 1-5, wherein at least one of said particles is a chromophore/luminophore.

23. The assembly of claim 22, wherein said chromophore/luminophore is selected from the group consisting of organic dyes, inorganic dyes, fluorophores, phosphophores, light absorbing nanoparticles, combinations thereof, and the metalated complexes thereof.

24. The assembly of claim 23, wherein said chromophore/luminophore is an organic dye selected from the group consisting of coumarins, pyrene, cyanines, benzenes, N-methylcarbazole, erythrosin B, N-acetyl-L-tryptophanamide, 2,5-diphenyloxazole, rubrene, and N-(3-sulfopropyl)acridinium.

25. The assembly of claim 23, wherein said chromophore/luminophore is an inorganic dye selected from the group consisting of porphyrins, phthalocyanines, chlorins, and metalated chromophores.

26. The assembly of claim 25, wherein said porphyrins are selected from the group consisting of tetra carboxy-phenyl-porphyrin (TCPP) and Zn-TCPP.

27. The assembly of claim 25, wherein said chromophore/luminophore is a metalated chromophore selected from the group consisting of ruthenium polypyridyl complexes, osmium polypyridyl complexes, rhodium polypyridyl complexes, 3-(1-methylbenzoimidazol-2-yl)-7-(diethylamino)-coumarin complexes of iridium(III), and 3-(benzothiazol-2-yl)-7-(diethylamino)-coumarin complexes with iridium(III).

28. The assembly of claim 23, said chromophore/luminophore is a fluorophore or phosphophor selected from the group consisting of phosphorescent dyes, fluoresceines, rhodamines, and anthracenes.

29. The assembly of any one of claims 1-5, wherein at least one of said particles is a quantum dot.

30. The assembly of claim 29, wherein said quantum dot is selected from the group consisting of CdSe/ZnS core/shell quantum dots, CdTe/CdSe core/shell quantum dots, CdSe/ZnTe core/shell quantum dots, and alloyed semiconductor quantum dots.

31. The assembly of any one of claims 29-30, wherein said quantum dot is less than about 10 nm in diameter.

32. The assembly of any one of claims 29-31, wherein said quantum dot is a stabilized quantum dot comprising resorcinarene ligands surrounding said quantum dot.

33. The assembly of any one of claims 1-32, wherein said linkage is comprised of an oligopeptide containing said consensus sequence.

34. The assembly of claim 33, wherein said oligopeptide comprises a hydrophilic region of at least 10 amino acids N-terminal to the protease cleavage region and a linking region C-terminal to the protease cleavage region.

35. The assembly of claim 34, wherein the C-terminal linking region comprises a thiol reactive group at its terminus.

36. The assembly of claim 34, wherein the C-terminal linking region comprises a cysteine residue, lysine, or aspartate.

37. The assembly of claim 34, wherein the C-terminal linking region comprises a sequence selected from the group consisting of GGGC (SEQ ID NO: 14), AAAC (SEQ ID NO: 15), SSSC (SEQ ID NO: 16), TTTC (SEQ ID NO: 17), GGC (SEQ ID NO: 38), GGK (SEQ ID NO: 39), GC (SEQ ID NO: 40), and GGD (SEQ ID NO: 42).

38. The assembly of claim 34, wherein the N-terminal region comprises a sequence selected from the group consisting of SRSRSRSRSR (SEQ ID NO: 1), KSRSRSRSRSR (SEQ ID NO: 19), KKSRSRSRSRSR (SEQ ID NO: 20), CGGG (SEQ ID NO: 23), KGGG (SEQ ID NO: 24), and KGG (SEQ ID NO: 37).

39. The assembly of any one of claims 34-38, wherein said N-terminal region further comprises at least one terminal group selected from the group consisting of lysine, ornithine, 2,4 diaminobutyric acid, and 2,3 diaminoproprionic acid.

40. The assembly of any one of claims 1-39, wherein said consensus sequence is selected from the group consisting of a serine protease cleavage sequence, an aspartate protease cleavage sequence, a cysteine protease cleavage, and a metalloprotease cleavage sequence.

41. The assembly of any one of claims 1-40, wherein said consensus sequence is selected from the group consisting of SGRSA (SEQ ID NO: 2), VPMSMRGG (SEQ ID NO: 3), IPVSLRSG (SEQ ID NO: 4), RPFSMIMG (SEQ ID NO: 5), VPLSLTMG (SEQ ID NO: 6), VPLSLYSG (SEQ ID NO: 7), IPESLRAG (SEQ ID NO: 8), SGSPAFLAKNR (SEQ ID NO: 9), DAFK (SEQ ID NO: 10), SGKPILFFRL (SEQ ID NO: 11), SGKPIIFFRL (SEQ ID NO:12), GPLGMLSQ (SEQ ID NO:13), HGPEGLRVGFYESDVMGRGHARLVHVEEPHT (SEQ ID NO: 25), GPQGLAGQRGIV (SEQ ID NO: 26), SLLKSRMVPNFN (SEQ ID NO: 27), SLLIFRSWANFN (SEQ ID NO: 28), and SGVVIATVIVIT (SEQ ID NO: 29).

42. The assembly of any one of claims 1-40, wherein said linkage is selected from the group consisting of SRSRSRSRSRSGRSAGGGC (SEQ ID NO: 18), KGGVPMSMRGGGC (SEQ ID NO: 30), KGGIPVSLRSGGC (SEQ ID NO: 31), KGGVPLSLTMGGC (SEQ ID NO: 32), KGGGSGRSAGGGC (SEQ ID NO: 33), CGGGSGRSAGGC (SEQ ID NO: 34), CGGGSGRSAGGGC (SEQ ID NO: 35), DGGSGRSAGGK (SEQ ID NO: 36), and KGGSGRSAGGD (SEQ ID NO: 41).

43. The assembly of any one of claims 1-21 and 33-42, wherein said first and second particles are both nanoparticles.

44. The assembly of claim 43, wherein said first and second particles are different nanoparticles.

45. The assembly of any one of claims 1-5, 22-28, and 33-42, wherein said first and second particles are both chromophores/luminophores.

46. The assembly of claim 45, wherein said first and second particles are different chromophores/luminophores.

47. The assembly any one of claims 45-46, wherein said linkage further comprises a spacer moiety attached to one of said particles.

48. The assembly of claim 47, wherein said spacer moiety comprises reactive groups selected from the group consisting of carboxyls, thiols, and combinations thereof.

49. The assembly of any one of claims 47-48, wherein said spacer moiety is covalently attached to the N-terminal region of said oligopeptide through an amide bond.

50. The assembly of any one of claims 47-48, wherein said spacer moiety is covalently attached to the C-terminal linking region of said oligopeptide through a disulfide bond.

51. The assembly of any one of claims 47-50, wherein said spacer moiety is selected from the group consisting of ethylene glycols, amides, alkylenes, and esters, each having two terminal carboxyl groups or a terminal carboxyl group and a terminal thiol group.

52. The assembly of any one of claims 1-4, 6-28, and 33-42, wherein said first particle is a nanoparticle and said second particle is a chromophore/luminophore.

53. The assembly of any one of claims 1-4, 6-21, and 29-42, wherein said first particle is a nanoparticle and said second particle is a quantum dot.

54. The assembly of any one of claims 1-53, wherein said first and second particles are separated by a distance that enables Förster resonance energy transfer or surface plasmon resonance between said first and second particles.

55. The assembly of any one of claims 52 and 53, wherein said first and second particles are separated by a distance that enables said first particle to quench the excited state of said second particle.

56. The assembly of any one of claims 54 and 55, wherein said first and second particles are separated by a distance of less than about 10 nm.

57. The assembly of any of the claims 1-56, further comprising up to 9 additional particles, each of said additional particles being linked to said first particle by respective linkages, wherein each of said linkages comprises a protease consensus sequence.

58. The assembly of claim 57, wherein the respective linkages between each of said additional particles and said first particle each comprises a different protease consensus sequence.

59. The assembly of any one of claims 57-58, wherein said additional particles are selected from the group consisting of chromophores/luminophores and quantum dots.

60. The assembly of any one of claims 57-59, wherein said first particle is selected from the group consisting of nanoparticles.

61. A composition comprising a diagnostic assay including the assembly of any one of claims 1 to 60 and a pharmaceutically-acceptable carrier.

62. The composition of claim 61, wherein said pharmaceutically-acceptable carrier is selected from the group consisting of an aqueous buffer and liposomes.

63. The composition of claim 62, wherein said liposome is from about 100 nm to about 5 μm.

64. The compositions of any one of claims 62-63, wherein said liposome comprises a phospholipid bilayer and cholesterol.

65. The compositions of any one of claims 62-64, wherein said liposome is thermolabile.

66. The composition of claim 65, wherein said liposome comprises N-isopropyl-acrylamide.

67. The composition of any one of claims 62-66, wherein said liposome further comprises a tumor-specific antibody or an aptamer.

68. A method for detecting the activity of a protease associated with a cancerous or precancerous cell in a mammal, said method comprising:

(a) contacting a fluid sample from the mammal with a diagnostic assay, said assay comprising the nanoplatform assembly of any one of claims 1-60;

(b) exposing said assay to an energy source; and

(c) detecting the changes in the absorption or emission spectrum of the assay, wherein said changes correspond to protease activity.

69. The method of claim 68, wherein said energy source is selected from the group consisting of a tungsten lamp, laser diode, laser, bioluminescence, and combinations thereof.

70. The method of any one of claims 68-69, wherein said exposing occurs at a wavelength of from about 400 nm to about 1000 nm.

71. The method of any one of claims 68-69, wherein said exposing occurs at a wavelength of from about 500 nm to about 1000 nm.

72. The method of any one of claims 68-71, wherein said fluid sample is selected from the group consisting of urine and blood.

73. The method of any one of claims 68-72, wherein a blue-shift in the absorption or emission maximum of the assay after contact with the fluid sample relative to the absorption or emission spectrum of the assay prior to contact with said fluid sample indicates the presence of a cancerous or precancerous cell in the mammal.

74. The method of any one of claims 68-73, wherein a blue-shift in absorption or emission spectrum maximum between about 5 nm and about 200 nm indicates the presence of a cancerous or precancerous cell in the mammal.

75. The method of any one of claims 68-72, wherein said change comprises the appearance of a new visible color or luminescence band relative to the absorption or emission spectrum of said assay prior to contact with said fluid sample, said visible color or luminescence band indicating the presence of a cancerous or precancerous cell in the mammal.

76. The method of any one of claims 68-75, wherein said changes in the absorption or emission spectrum of said assay are observed over a time period of from about 1 second to about 30 minutes.

77. The method of any one of claims 68-76, wherein said change in absorption or emission spectrum indicates the activity of a protease selected from the group consisting of uPA, MMP-1, MMP-2, MMP-7, and combinations thereof.

78. The method of claim 77, further comprising correlating said protease activity with a prognosis for cancer progression.

79. The method of claim 78, wherein the detection of activity of both uPA and MMP-7, and absence of activity of both MMP-1 and MMP-2, is correlated with a prognosis for angiogensis.

80. The method of claim 78, wherein the detection of activity of all of uPA, MMP-1, MMP-2, MMP-7 is correlated with a prognosis for cell invasion.

81. A method for detecting the activity of a protease associated with a cancerous or precancerous cell in a mammal comprising:

(a) administering to the mammal the composition of any one of claims 61-67;

(b) activating the assay in said composition;

(c) exposing a region of the mammal suspected of having a cancerous or precancerous cell to an energy source; and

(d) detecting the changes in the absorption or emission spectrum of the assay, wherein said changes correspond to protease activity.

82. The method of claim 81, wherein said administering (a) comprises injecting said composition directly into said region of the mammal suspected of having a cancerous or precancerous cell.

83. The method of claim 81, wherein said administering (a) comprises injecting said composition into the bloodstream of said mammal.

84. The method of claim 83, wherein said composition reaches said region suspected of having a cancerous or precancerous cell within one hour after injection.

85. The method of any one of claims 81-84, wherein said activating (b) comprises heating said assay to a temperature sufficient to release said assay from said pharmaceutically-acceptable carrier.

86. The method of claim 85, wherein said heating comprises photophysical heating of said assay.

87. The method of any one of claims 85-86, wherein said heating causes thermocollapse of said pharmaceutically-acceptable carrier.

88. The method of any one of claims 81-84, wherein said energy source is selected from the group consisting of a tungsten lamp, laser diode, laser, bioluminescence, and combinations thereof.

89. The method of any one of claims 81-88, wherein said exposing occurs at a wavelength of from about 400 nm to about 500 nm or from about 800 nm to about 900 nm.

90. The method of any one of claims 81-89, wherein a blue-shift in absorption or emission spectrum maximum between about 5 nm and about 200 nm indicates the presence of a cancerous or precancerous cell in the mammal.

91. The method of any one of claims 81-89, wherein said change comprises the appearance of a new luminescence band relative to the absorption or emission spectrum of said assay prior to said activating (b), said luminescence band indicating the presence of a cancerous or precancerous cell in the mammal.

92. The method of claim 81, further comprising correlating said protease activity with a prognosis for cancer progression.

93. The method of any one of claims 81-92, wherein protease activity detected within 10 minutes after activating said assay is correlated with a high probability that the cancerous or precancerous cell is aggressive.

94. The method of any one of claims 81-92, wherein the absence of protease activity detection within the first 30 minutes after activating said assay is correlated with a very low probability that the cancerous or precancerous cell is aggressive.

95. The method of any one of claims 81-94, wherein a change in absorption or emission spectrum indicates the activity of a protease selected from the group consisting of uPA, MMP-1, MMP-2, MMP-7, and combinations thereof.

96. The method of claim 95, wherein the detection of activity of both uPA and MMP-7, and the absence of activity of both MMP-1 and MMP-2, is correlated with a prognosis for angiogensis.

97. The method of claim 95, wherein the detection of activity of all of uPA, MMP-1, MMP-2, MMP-7 is correlated with a prognosis for cell invasion.

98. The method of claim 81, wherein said protease activity results in two or more oligopeptide sequences selected from the group consisting of KGGVPMS (SEQ ID NO: 43), MRGGGC (SEQ ID NO: 44), KGGIPVS (SEQ ID NO: 45), LRSGGC (SEQ ID NO: 46), KGGVPLS (SEQ ID NO: 47), LTMGGC (SEQ ID NO: 48), KGGGSGR (SEQ ID NO: 49), SAGGGC (SEQ ID NO: 50), CGGGSGR (SEQ ID NO: 51), SAGGC (SEQ ID NO: 52), DGGSGR (SEQ ID NO: 53), SAGGK (SEQ ID NO: 54), SRSRSRSRSRSGR (SEQ ID NO: 55), KGGSGR (SEQ ID NO: 56), and SAGGD (SEQ ID NO: 57).

99. The method of any one of claims 68 to 98, wherein said cancerous or precancerous cell is associated with a cancer selected fro the group consisting of an AIDS-related cancer, AIDS-related lymphoma, anal cancer, appendix cancer, childhood cerebellar astrocytoma, childhood cerebral astrocytoma, basal cell carcinoma, extrahepatic bile duct cancer, childhood brain stem glioma, adult brain tumor, childhood malignant glioma, childhood ependymoma, childhood medulloblastoma, childhood supratentorial primitive neuroectodermal tumors, childhood visual pathway and hypothalamic glioma, breast cancer, pregnancy-related breast cancer, childhood breast cancer, male breast cancer, childhood carcinoid tumor, gastrointestinal carcinoid tumor, primary central nervous system lymphoma, cervical cancer, colon cancer, childhood colorectal cancer, esophageal cancer, childhood esophageal cancer, intraocular melanoma, retinoblastoma, adult glioma, adult (primary) hepatocellular cancer, childhood (primary) hepatocellular cancer, adult Hodgkin lymphoma, childhood Hodgkin lymphoma, islet cell tumors, Kaposi Sarcoma, kidney (renal cell) cancer, childhood kidney cancer, adult (primary) liver cancer, childhood (primary) liver cancer, Non-small cell liver cancer, small cell liver cancer, AIDS-related lymphoma, Burkitt lymphoma, adult Non-Hodgkin lymphoma, childhood Non-Hodgkin lymphoma, primary central nervous system lymphoma, melanoma, adult malignant mesothelioma, childhood mesothelioma, metastatic squamous neck cancer with occult primary, mouth cancer, childhood multiple endocrine neoplasia syndrome, multiple myeloma/plasma cell neoplasm, mycosis fungoides, myelodysplastic syndromes, myelodysplastic/myeloproliferative diseases, adult acute myeloid leukemia, childhood acute myeloid leukemia, multiple myeloma, neuroblastoma, non-small cell lung cancer, childhood ovarian cancer, ovarian epithelial cancer, ovarian germ cell tumor, ovarian low malignant potential tumor, pancreatic cancer, childhood pancreatic cancer, islet cell pancreatic cancer, parathyroid cancer, penile cancer, plasma cell neoplasm/multiple myeloma, pleuropulmonary blastoma, prostate cancer, rectal cancer, childhood renal cell cancer, renal pelvis and ureter, transitional cell cancer, adult soft tissue sarcoma, childhood soft tissue sarcoma, uterine sarcoma, skin cancer (nonmelanoma), childhood skin cancer, melanoma, Merkel cell skin carcinoma, small cell lung cancer, small intestine cancer, squamous cell carcinoma, stomach cancer, childhood stomach cancer, cutaneous T-Cell lymphoma, testicular cancer, thyroid cancer, childhood thyroid cancer, and vaginal cancer.

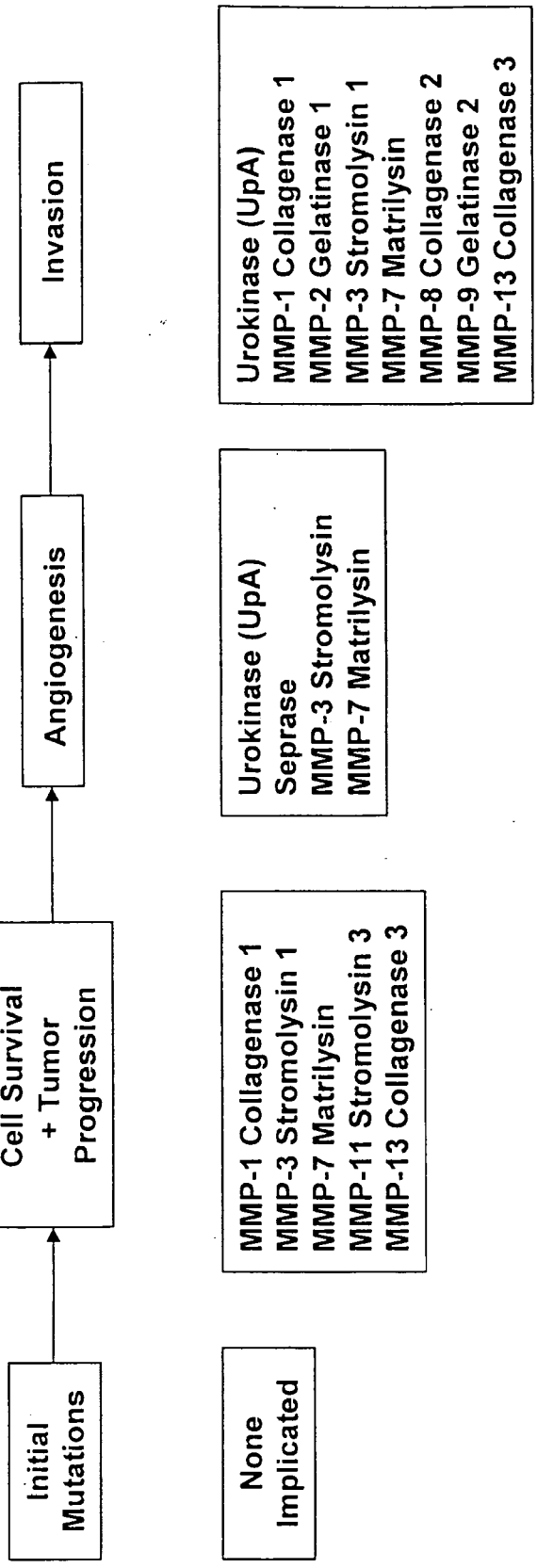
Initial Mutations
Cell Survival + Tumor Progression
Angiogenesis
Invasion
None Implicated
MMP-1 Collagenase 1
MMP-3 Stromolysin 1
MMP-7 Matrilysin
MMP-11 Stromolysin 3
MMP-13 Collagenase 3
Urokinase (UpA)
Seprase
MMP-3 Stromolysin
MMP-7 Matrilysin
Urokinase (UpA)
MMP-1 Collagenase 1
MMP-2 Gelatinase 1
MMP-3 Stromolysin 1
MMP-7 Matrilysin
MMP-8 Collagenase 2
MMP-9 Gelatinase 2
MMP-13 Collagenase 3

Fig. 1

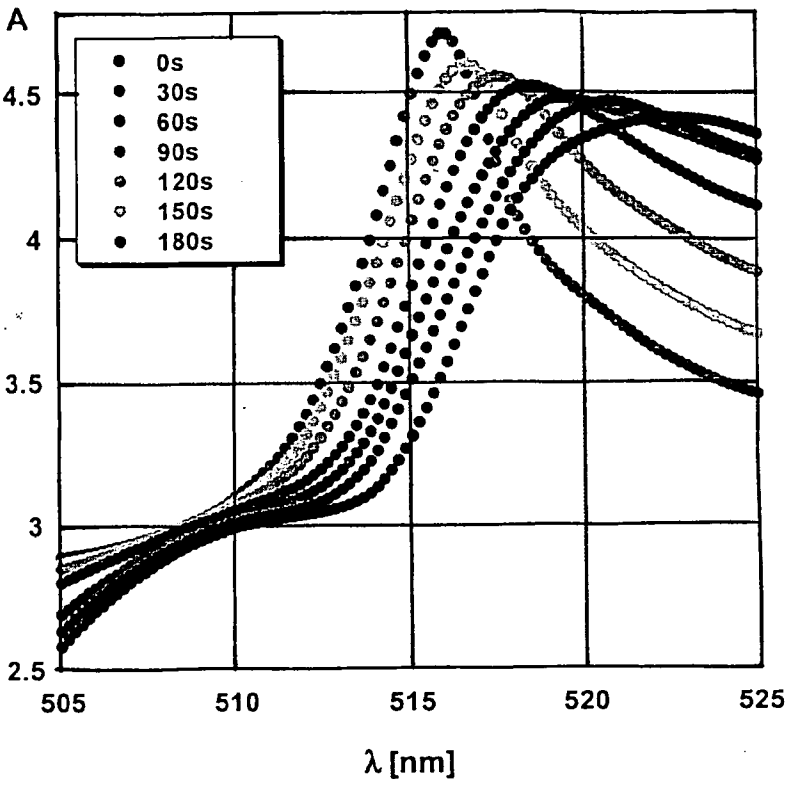
A
4.5
4
3.5
3
2.5
505
510
515
520
525
λ [nm]
0s
30s
60s
90s
120s
150s
180s

Fig. 2

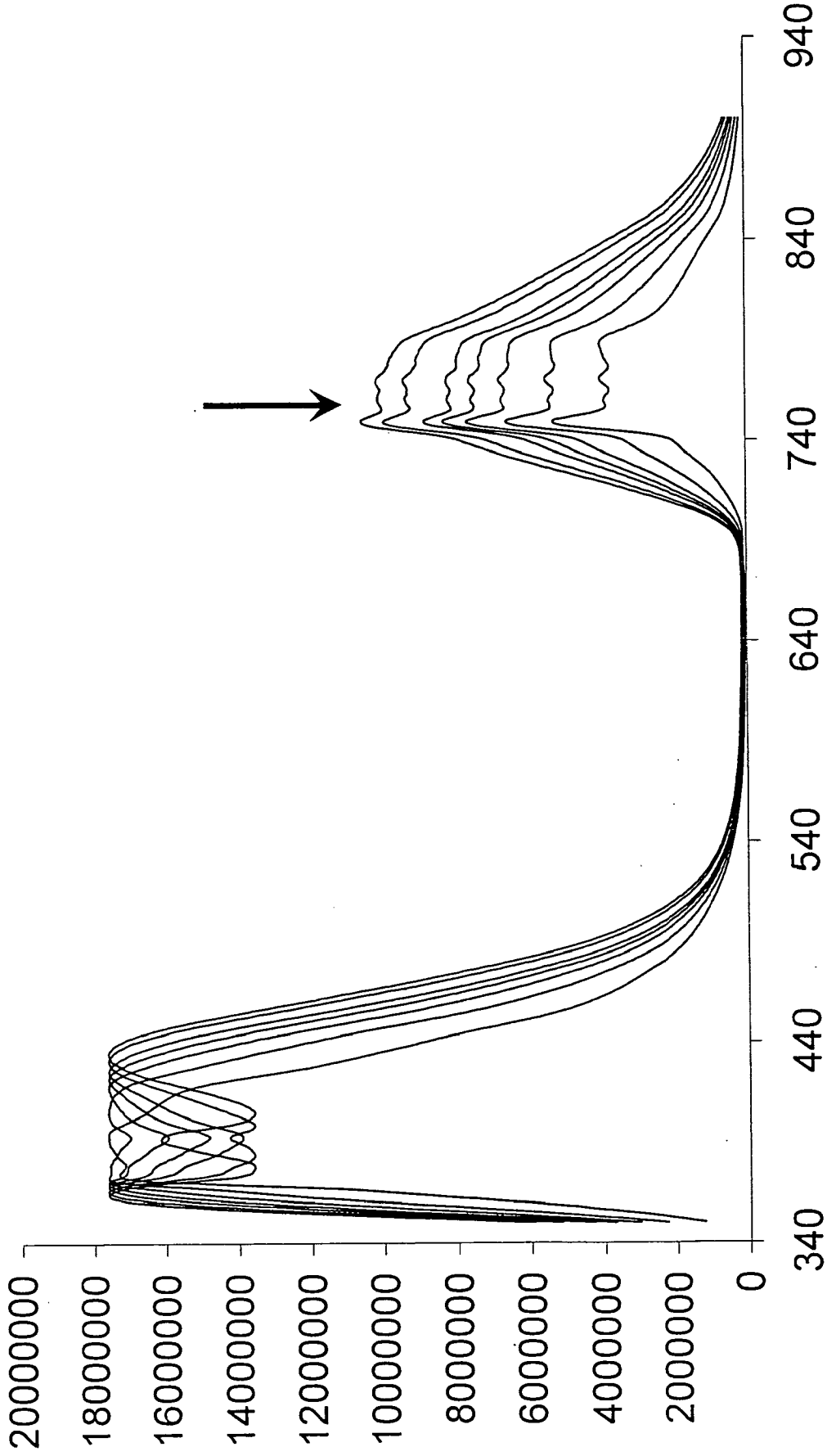
20000000
18000000
16000000
14000000
12000000
10000000
8000000
6000000
4000000
2000000
0
340
440
540
640
740
840
940
λ / nm

Fig. 3

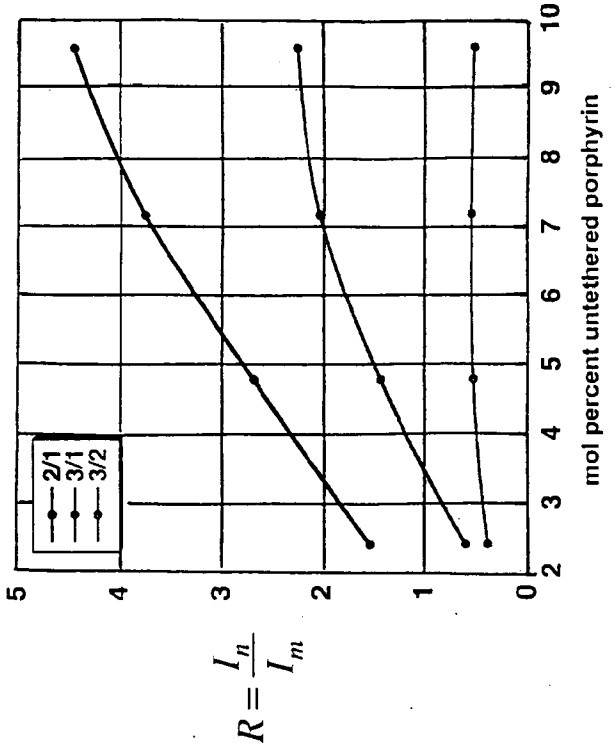
2/1
3/1
3/2
mol percent untethered porphyrin
$R = \frac{I_n}{I_m}$

Fig. 5

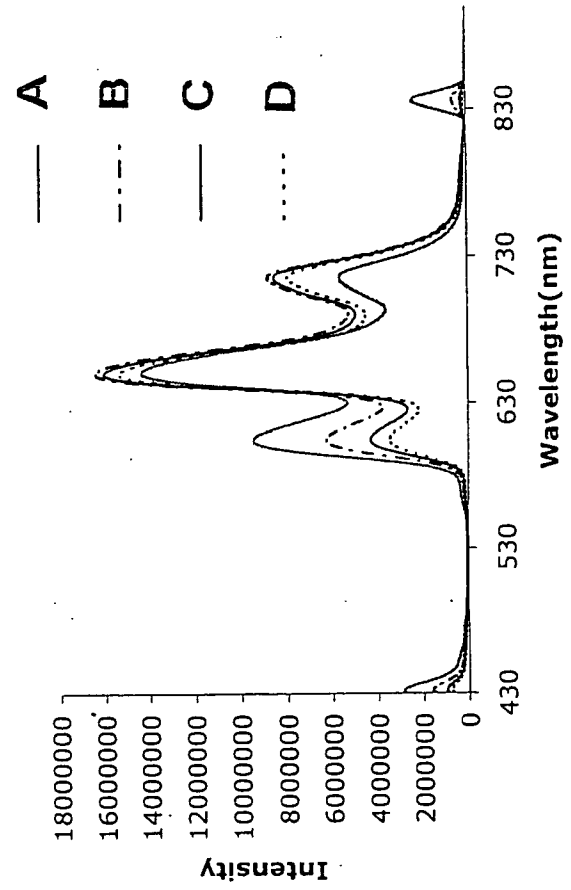
A
B
C
D
Intensity
Wavelength(nm)

Fig. 4

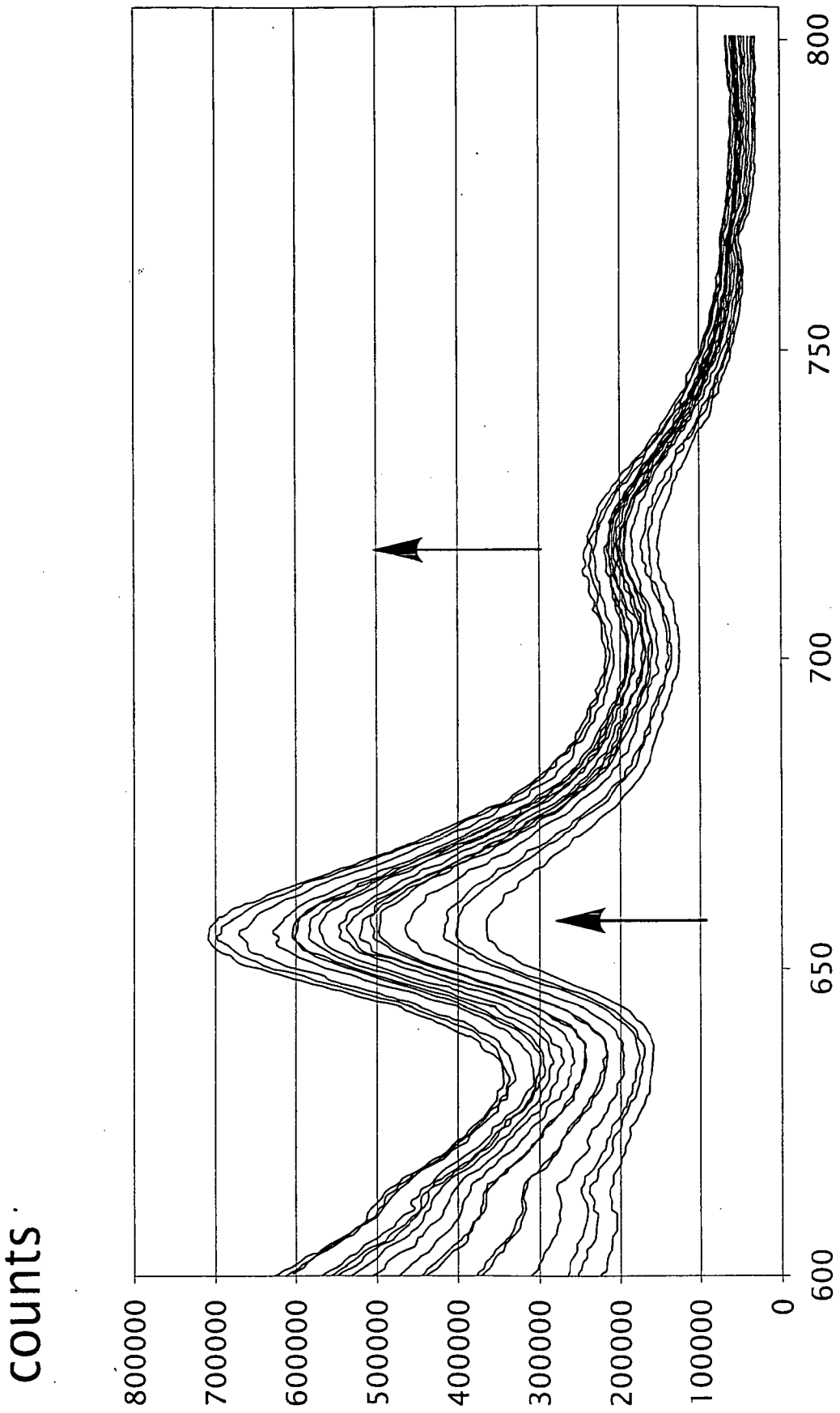
counts
800000
700000
600000
500000
400000
300000
200000
100000
0
600
650
700
750
800
nm

Fig. 6

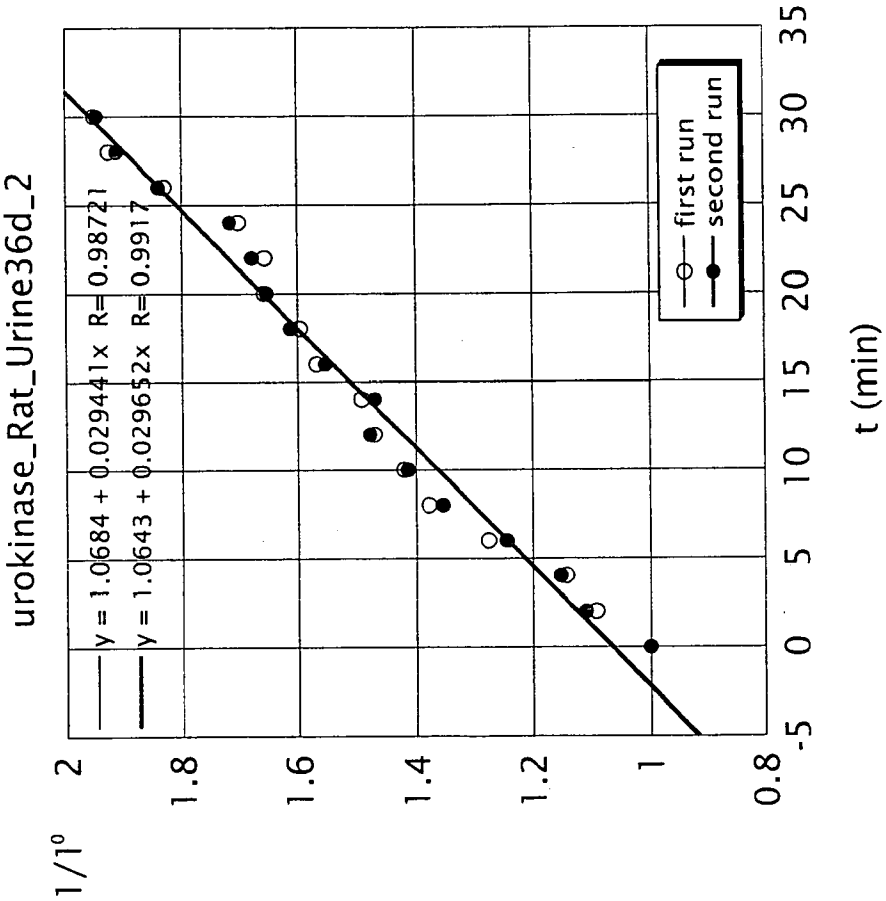
urokinase_Rat_Urine36d_2
y = 1.0684 + 0.029441x R= 0.98721
y = 1.0643 + 0.029652x R= 0.9917
first run
second run
1/I°
t (min)
2
1.8
1.6
1.4
1.2
1
0.8
-5
0
5
10
15
20
25
30
35

Fig. 7

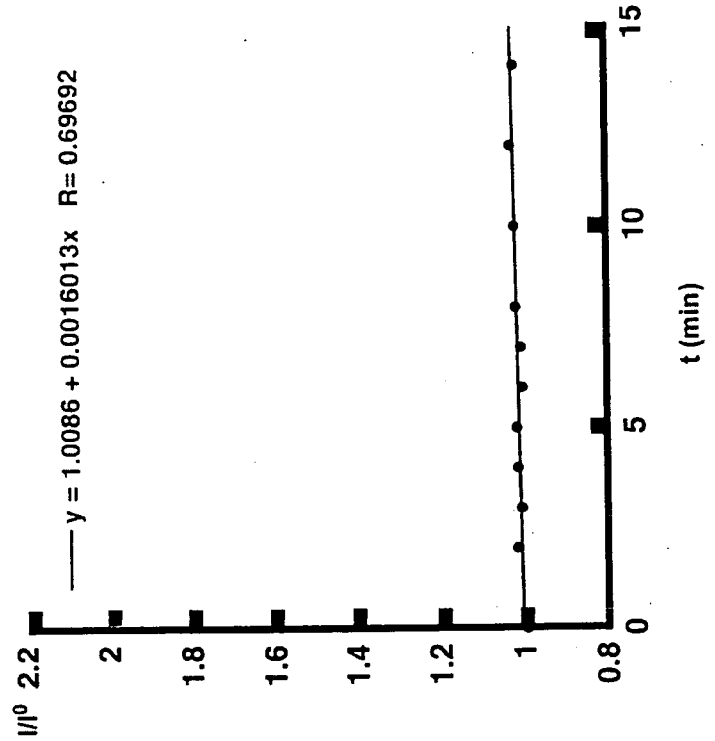
y = 1.0086 + 0.0016013x R= 0.69692
I/I0
t (min)
2.2
2
1.8
1.6
1.4
1.2
1
0.8
0
5
10
15

Fig. 9

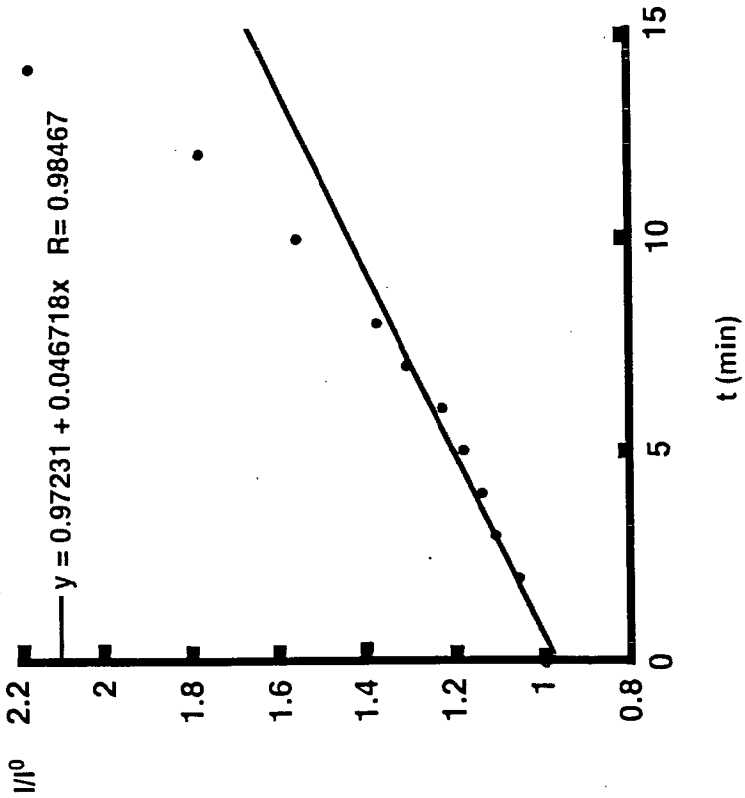
y = 0.97231 + 0.046718x R= 0.98467
I/I0
t (min)
2.2
2
1.8
1.6
1.4
1.2
1
0.8
0
5
10
15

Fig. 8

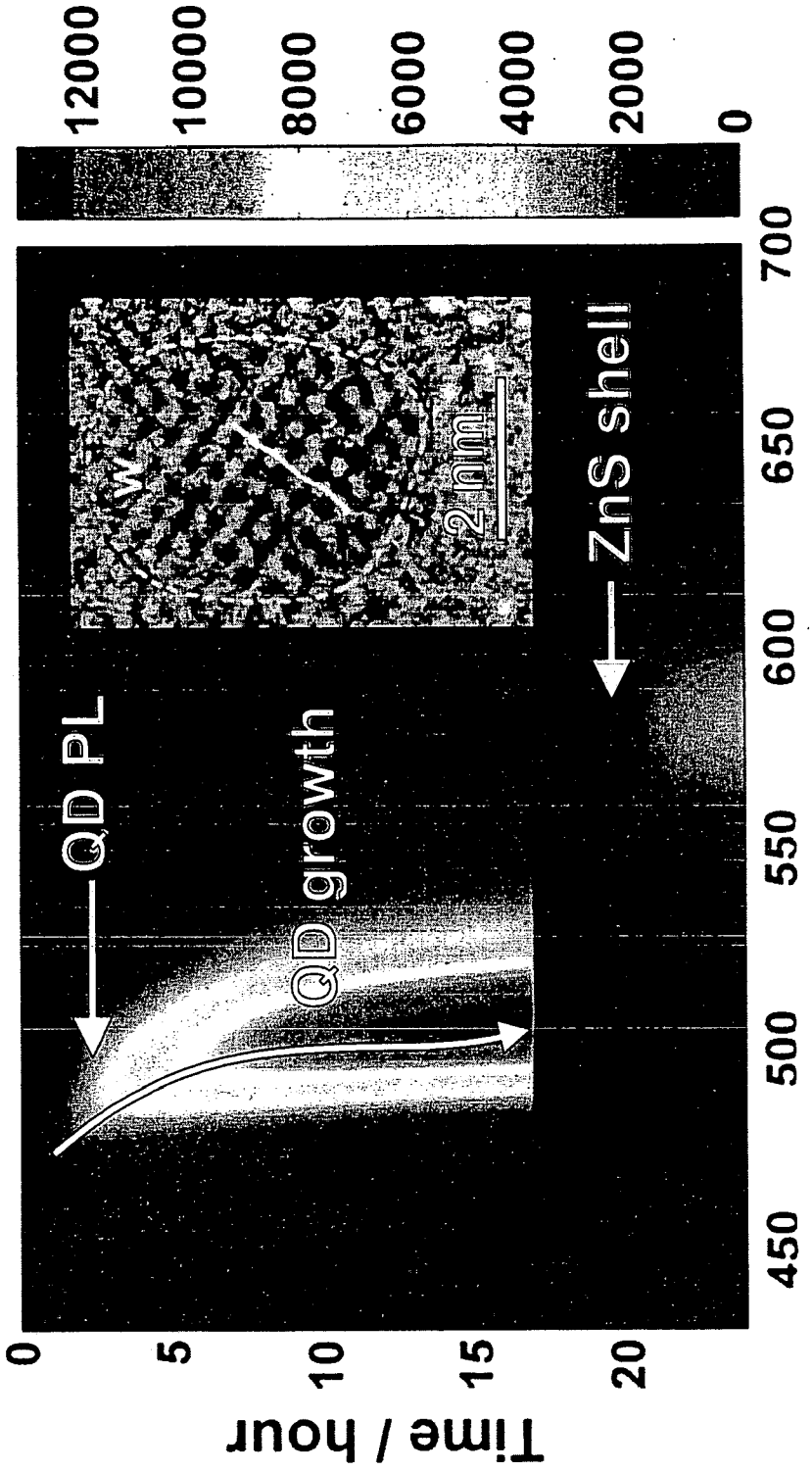
12000
10000
8000
6000
4000
2000
0
700
650
600
550
500
450
0
5
10
15
20
Time / hour
QD PL
QD growth
ZnS shell
2 nm

Fig. 10

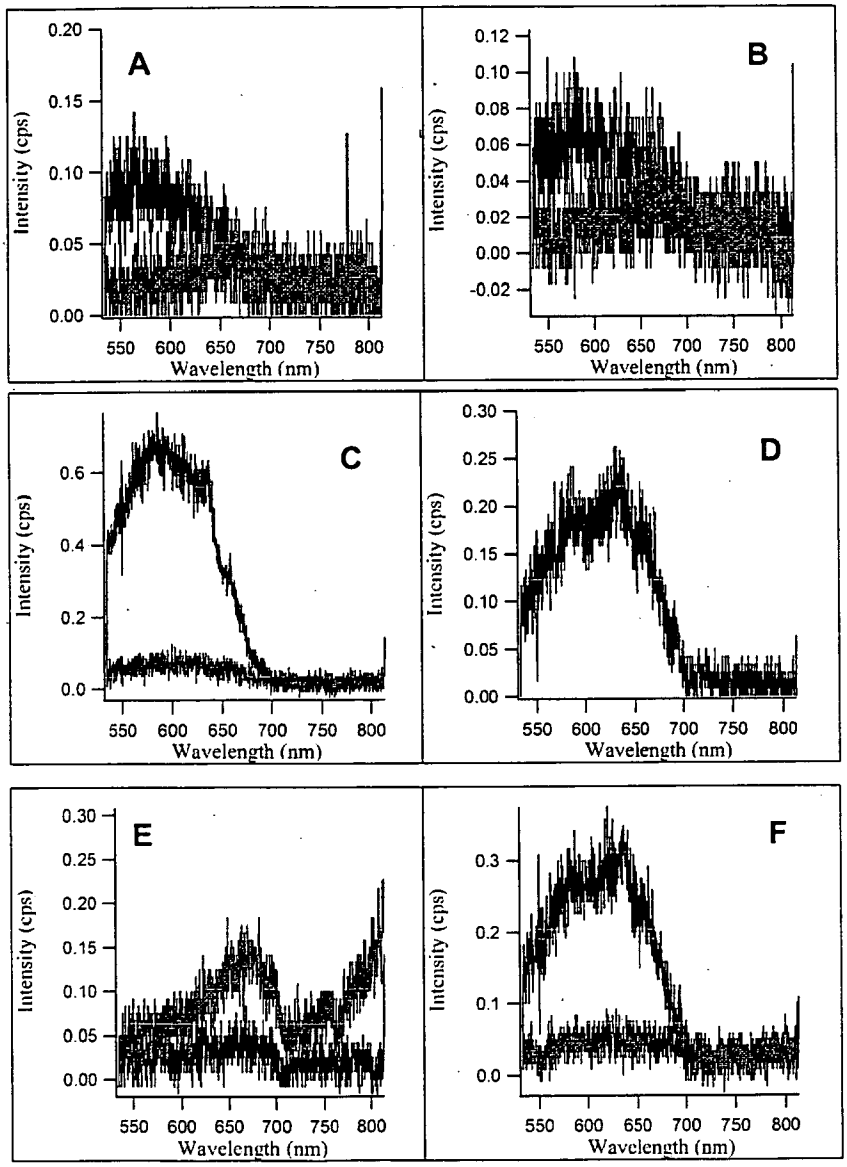

Fig. 11

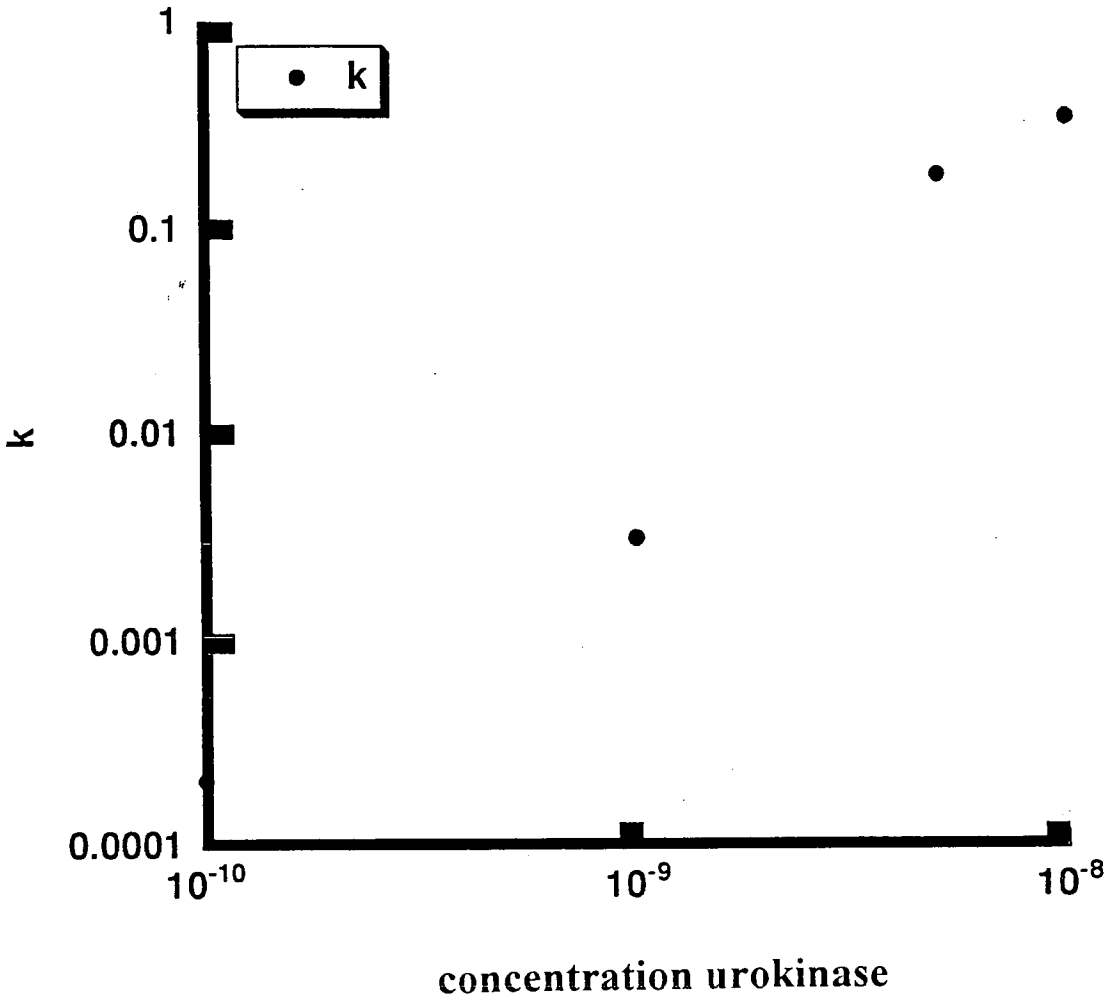

Fig. 12

专利名称(译)	蛋白酶测定		
公开(公告)号	EP2260108A2	公开(公告)日	2010-12-15
申请号	EP2009718303	申请日	2009-03-03
申请(专利权)人(译)	堪萨斯州立大学研究基金会		
当前申请(专利权)人(译)	堪萨斯州立大学研究基金会		
[标]发明人	BOSSMANN STEFAN H TROYER DERYL L BASEL MATTHEW T		
发明人	BOSSMANN, STEFAN, H. TROYER, DERYL, L. BASEL, MATTHEW, T.		
IPC分类号	C12Q1/37 B82B1/00 G01N33/53 G01N33/543 A61K33/26		
CPC分类号	A61K49/0067 A61K49/0036 A61K49/0056 A61K49/0065 A61K49/0093 B82Y15/00 C07K5/1021 C07K7/06 C07K7/08 C12Q1/37 G01N33/588 G01N2800/7028 Y10S977/773 Y10S977/774 Y10S977/92		
代理机构(译)	UEXKÜLL & STOLBERG		
优先权	61/067891 2008-03-03 US		
其他公开文献	EP2260108B1 EP2260108A4		
外部链接	Espacenet		

摘要(译)

本发明提供了用于评估体内或体外蛋白酶活性的诊断试剂或测定法以及检测癌细胞或癌前细胞存在的方法。该测定由两个通过寡肽键连接的颗粒组成，该寡肽键包含对靶蛋白酶特异的共有序列。可以通过目测或使用各种传感器检测靶蛋白酶对序列的切割，并且诊断结果可以与癌症预后相关联。